895. Combination resonance analysis of a multi-DOF controllable close-chain linkage mechanism system

Rugui Wang[1], Guanglin Shi[2], Ganwei Cai[3], Xiaorong Zhou[4]
[1, 3, 4]College of Mechanical Engineering, Guangxi University, Nanning 530004, China
[2]Department of Mechanical Engineering, Guangxi University of Technology, Liuzhou, 545006, China
E-mail: [1]*rugui@163.com*, [2]*sgl8913@163.com*, [3]*caiganwei@163.com*, [4]*xrzhou@gxu.edu.cn*

(Received 17 August 2012; accepted 4 December 2012)

Abstract. The two-DOF controllable close-chain linkage mechanism system is investigated in this paper. Based on the air-gap field of the non-uniform airspace of motors caused by the eccentricity of rotor, the electromechanical coupling relation in the real running state of motors is analyzed. The electromechanical coupling dynamic model of the system is established by means of the finite element method. The dynamic equation constitutes the basis on which the combination resonance characteristics of the system caused by electromagnetic parameter excitations of the two motors are analyzed by the multiple scales method. The first-order stationary solution is obtained under that condition, and the stability conditions of the stationary solution are also given. Finally, an experiment is presented. Results indicate that it is feasible and beneficial to explain some unexpected strong vibration phenomena in the high-speed operation of such multi-DOF controllable close-chain linkage mechanism using nonlinear combination resonance theories.

Keywords: multi-DOF controllable close-chain linkage mechanism, combination resonance, electromagnetic parameter excitation.

Introduction

Multi-DOF controllable close-chain linkage mechanism, which can accurately actualize given random trajectory, velocity and acceleration, has a wide outlook of application in robots, automatic production lines, etc. [1, 2]. The application and study of modern mechanisms indicate that the studies on the dynamic characteristics are necessary for mechanisms to carry out high speed, high precision and low noise operation. Many scholars have widely studied the nonlinear dynamics of elastic linkage mechanisms by different methods for their different purposes. Liou [3], Ahmad Smaili [4] and Liu [5] et al. have studied the dynamic behaviors of a DC motor single-DOF linkage mechanism system. But their analysis is based on the motor having no eccentric vibration and treating the motor air-gap field as steady and uniform, and the electromechanical coupling relation considered in the real running state of motor is oversimplified. Li [6] has analyzed the nonlinear dynamics of three-phase AC motor-linkage mechanism system. However, the studies aimed at the dynamic characteristics of the single-DOF linkage mechanism, which only achieves simple fixed motion curve, and is rarely used. The studies on dynamic characteristics of widely used multiple-DOF controllable linkage mechanisms have not been extensively performed, and some unexpected vibration characteristics of such kind of linkage mechanism system cannot be explained. For example, the sub-harmonic resonance, super-harmonic resonance and combination resonance may occur in the system under certain conditions.

The 2-DOF controllable close-chain linkage mechanism is investigated in this paper (Fig. 1). The dynamic equation is the basis on which the combination resonance properties of the system caused by electromagnetic parameter excitations of the two controllable motors are analyzed. The work presented in this paper is beneficial for further studies on the inner connections between dynamic characteristics and motor electromagnetism parameters of the mechanism system. And the results indicate that it is feasible to explain some unexpected strong vibration

phenomena in the high-speed operation of such Multi-DOF controllable close-chain linkage mechanism using nonlinear combination resonance theories.

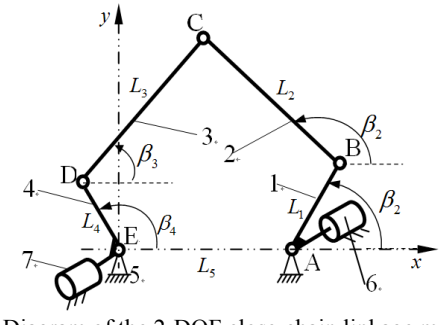

Fig. 1. Diagram of the 2-DOF close-chain linkage mechanism:
1 - crank, 2 - coupler, 3 - coupler, 4 - crank, 5 - frame, 6 - motor 1, 7 - motor 2

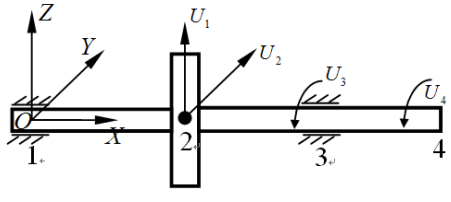

Fig. 2. Diagram of the controllable motor element

Dynamic model of the 2-DOF controllable close-chain linkage mechanism system

The linkage mechanism and the two controllable motors constitute an integrated system. The two controllable motors are servomotor (motor 1) and 3-phase AC motor (motor 2). Thereby, a 2-DOF close-chain linkage mechanism is derived by hybrid motors. Based on the air-gap field of non-uniform airspace of controllable motors of the close-chain linkage mechanism caused by the eccentricity of rotor, the controllable motor element [7, 8] as shown in Fig. 2, which defines the transverse vibration and torsional vibration of the controllable motors as its nodal displacement, are established. The electromechanical coupling relation in the real running state of motor was analyzed, and the kinetic energy, elastic potential energy and air-gap magnetic field potential energy of the controllable motor element are deduced. Then, the mass matrix and stiffness matrix of the controllable motor element in the local coordinate system are deduced respectively. In the element analysis of the mechanism, the links of linkage mechanism are simulated using beam element, and the mass matrix and stiffness matrix of the beam element are derived from the relationship between the strain distribution of each part and the node displacement of the beam element. An nonlinear electromechanical coupling dynamic model of the system, which includs electromagnetic parameters of the controllable motors and structural parameters of the system, was established by the finite element method as follows [8]:

$$\boldsymbol{M}\ddot{\boldsymbol{u}} + \boldsymbol{C}\dot{\boldsymbol{u}} + (\boldsymbol{K} + \boldsymbol{K}_0)\boldsymbol{u} = \boldsymbol{P} - \boldsymbol{M}\ddot{\boldsymbol{u}}_r - (\boldsymbol{K}_1^e + \boldsymbol{K}_2^e)\boldsymbol{e} - \boldsymbol{k}_0 + \varepsilon. \quad (1)$$

where, $\boldsymbol{u}$ is the generalized coordinates array of the system, $\boldsymbol{M}$ and $\boldsymbol{C}$ are respectively the $n \times n$ mass matrix and damping matrix of the system, $\boldsymbol{K}$ and $\boldsymbol{K}_1^e$ are the $n \times n$ stiffness matrixes in connection with the structural parameters of the system, $\boldsymbol{K}_0$ and $\boldsymbol{K}_2^e$ are the $n \times n$ stiffness

matrixes in connection with the electromagnetic parameters of the system, $\boldsymbol{k}_0$ is the n order array in connection with the electromagnetic parameters, $\boldsymbol{P}$ is the external force array of the system, $\ddot{\boldsymbol{u}}_r$ is the rigid acceleration array of system in the global coordinates, $\boldsymbol{e}$ is an array in connection with the eccentricity of rotor, ε is the nonlinear term, also is a small parameter, and:

$$\varepsilon=\sum_{n=1}^{8}\boldsymbol{u}^{\mathrm{T}}\boldsymbol{G}_n\boldsymbol{K}_n\boldsymbol{u}+\frac{1}{2}\sum_{n=1}^{8}\boldsymbol{u}^{\mathrm{T}}\boldsymbol{K}_n\boldsymbol{u}\boldsymbol{G}_n+\frac{1}{2}\sum_g\sum_l\boldsymbol{u}^{\mathrm{T}}\boldsymbol{G}_{gl}\boldsymbol{u}\boldsymbol{K}_{gl}\boldsymbol{u}+\frac{1}{2}\sum_g\sum_l\boldsymbol{G}_{gl}\boldsymbol{u}\boldsymbol{u}^{\mathrm{T}}\boldsymbol{K}_{gl}\boldsymbol{u},\quad (g,l=2,3,4,6,7,8). \tag{2}$$

$\boldsymbol{G}_n, \boldsymbol{K}_n, \boldsymbol{G}_{gl}$ and $\boldsymbol{K}_{gl}$ are the $n\times n$ matrixes in connection with the structural parameters of the linkage mechanism, and:

$$\boldsymbol{M}=\boldsymbol{B}_1^T\boldsymbol{R}_1^T\,\bar{\boldsymbol{M}}_1\,\boldsymbol{R}_1\boldsymbol{B}_1+\boldsymbol{B}_2^T\boldsymbol{R}_2^T\,\bar{\boldsymbol{M}}_2\,\boldsymbol{R}_2\boldsymbol{B}_2+\sum_{i=3}^{n}\boldsymbol{B}_i^T\boldsymbol{R}_i^T\,\bar{\boldsymbol{M}}_3\,\boldsymbol{R}_i\boldsymbol{B}_i,\ \boldsymbol{K}_0=\boldsymbol{K}_{12}^e+\boldsymbol{K}_{22}^e,$$

$$\boldsymbol{K}=\boldsymbol{K}_{11}^e+\boldsymbol{K}_{21}^e+\sum_{i=3}^{n}\boldsymbol{B}_i^T\boldsymbol{R}_i^T\,\bar{\boldsymbol{K}}_3\,\boldsymbol{R}_i\boldsymbol{B}_i,\ \boldsymbol{K}_1^e=\boldsymbol{K}_{11}^e+\boldsymbol{K}_{12}^e,\ \boldsymbol{K}_2^e=\boldsymbol{K}_{21}^e+\boldsymbol{K}_{22}^e,\ \boldsymbol{K}_{11}^e=\boldsymbol{B}_1^T\boldsymbol{R}_1^T\,\bar{\boldsymbol{K}}_{11}\,\boldsymbol{R}_1\boldsymbol{B}_1,$$

$$\boldsymbol{K}_{12}^e=\boldsymbol{B}_1^T\boldsymbol{R}_1^T\,\bar{\boldsymbol{K}}_{12}\,\boldsymbol{R}_1\boldsymbol{B}_1,\ \boldsymbol{K}_{21}^e=\boldsymbol{B}_2^T\boldsymbol{R}_2^T\,\bar{\boldsymbol{K}}_{21}\,\boldsymbol{R}_2\boldsymbol{B}_2,\ \boldsymbol{K}_{22}^e=\boldsymbol{B}_2^T\boldsymbol{R}_2^T\,\bar{\boldsymbol{K}}_{22}\,\boldsymbol{R}_2\boldsymbol{B}_2,$$

$$\boldsymbol{e}=\boldsymbol{B}_1^T\boldsymbol{R}_1^T\bar{\boldsymbol{e}}_1+\boldsymbol{B}_2^T\boldsymbol{R}_2^T\bar{\boldsymbol{e}}_2,\ \bar{\boldsymbol{e}}_1=[e_{11}+\varepsilon_{01}\cos\beta_1\quad e_{12}+\varepsilon_{01}\sin\beta_1\quad 0\quad 0]^T,$$

$$\bar{\boldsymbol{e}}_2=[e_{21}+\varepsilon_{02}\cos\beta_2\quad e_{22}+\varepsilon_{02}\sin\beta_2\quad 0\quad 0]^T,\ \boldsymbol{k}_0=\boldsymbol{B}_1^T\boldsymbol{R}_1^T\bar{\boldsymbol{k}}_{01}+\boldsymbol{B}_2^T\boldsymbol{R}_2^T\bar{\boldsymbol{k}}_{02},$$

$$\boldsymbol{G}_n=\sum_{i=3}^{N}\boldsymbol{B}_i^T\boldsymbol{R}_i^T\bar{\boldsymbol{g}}_n,\quad (\bar{\boldsymbol{g}}_n)_i=1,\quad (i=1,2\ldots,8),\ \boldsymbol{K}_n=\sum_{i=3}^{N}\boldsymbol{B}_i^T\boldsymbol{R}_i^T[\int_0^L EA\bar{\boldsymbol{g}}_n^T\bar{\boldsymbol{g}}\bar{\boldsymbol{K}}_a d\bar{x}]\boldsymbol{R}_i\boldsymbol{B}_i,$$

$$\bar{\boldsymbol{g}}=[-\frac{1}{L}\quad 0\quad 0\quad 0\quad \frac{1}{L}\quad 0\quad 0\quad 0]^T,\ (\bar{\boldsymbol{K}}_a)_{ij}=\gamma_i'\gamma_j',\quad i,j=2,3,4,6,7,8,$$

$$\boldsymbol{G}_{gl}=\sum_{i=3}^{N}\boldsymbol{B}_i^T\boldsymbol{R}_i^T\bar{\boldsymbol{G}}_{gl}\boldsymbol{R}_i\boldsymbol{B}_i,\ (\bar{\boldsymbol{G}}_{gl})_{gl}=(\bar{\boldsymbol{G}}_{gl})_{lg}=1,\quad g,l=2,3,4,6,7,8,\ \boldsymbol{K}_{gl}=\sum_{i=3}^{N}\boldsymbol{B}_i^T\boldsymbol{R}_i^T\bar{\boldsymbol{K}}_{gl}\boldsymbol{R}_i\boldsymbol{B}_i,$$

$(\bar{\boldsymbol{K}}_{gl})_{ij}=(\bar{\boldsymbol{K}}_{gl})_{ji}=\int_0^L EA\gamma_g'\gamma_l'\gamma_i'\gamma_j'd\bar{x},\quad i,j=2,3,4,6,7,8$, and N is the number of the element. γ_i are the shape functions (see the Appendix).

The air-gap eccentric vibration schematic diagram of the motor rotor is shown in Fig. 3, where point O is the inner circle geometric center of the motor stator, point O_1 is the outer circle geometric center of the rotor journal, point O_2 is the outer circle center of the journal under the deformation of shaft or bearing, and the coordinates of point $O_3(x,y)$ is the outer circle geometric center of the rotor, δ is the length of air gap, e_1 is the air-gap eccentricity. $e_{01}=\sqrt{e_{11}^2+e_{12}^2}$ is the static eccentricity, which is caused by the rotor gravity and mismatching tolerance of motor. ε_{01} is the rotational eccentricity, which is caused by centering error between the outer circle center of the journal and the outer circle geometric center of the rotor. The static eccentricity and the rotational eccentricity are considered at the same time in this paper. The static and rotational eccentricities can also be ignored, and only the eccentricity caused by rotor vibration be considered in engineering application. Then $e_1=\sqrt{x^2+y^2}$, and:

$$\begin{cases}x=U_1+e_{11}+\varepsilon_{01}\cos\beta_1\\ y=U_2+e_{12}+\varepsilon_{01}\sin\beta_1\end{cases} \tag{3}$$

where U_1 and U_2 are the component of vibration eccentricity in the x and y direction, and $e_0 = \sqrt{u_1^2 + u_2^2}$. $\beta_1 = (1 - s_1)\omega_{01} t$ is the rotational angle of rotor with respect to the stator of controllable motor. ω_{01} is the synchronous speed of rotation of controllable motor. s_1 is the slide ratio.

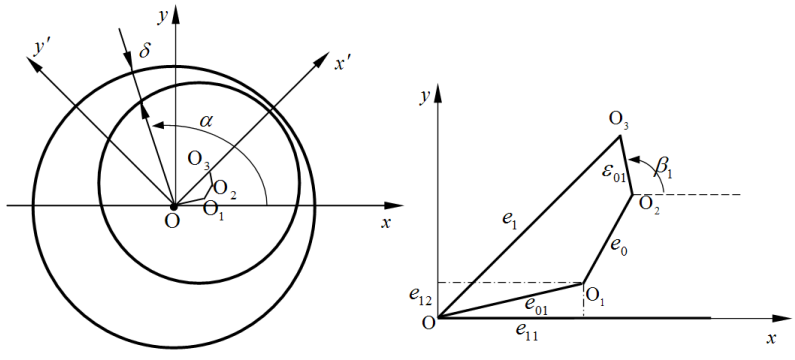

Fig. 3. Diagram of air-gap eccentric vibration of controllable motor

According to the theory of electromechanical analysis dynamics [9], the air-gap magnetic field potential energy of the controllable motor 1 (servomotor) is:

$$V_{12} = \frac{R_{01} l_{01} \Lambda_{01}}{2} \int_0^{2\pi} \{[(1 + \frac{x^2 + y^2}{2\sigma_1^2}) + \frac{x}{\sigma_1}\cos\alpha + \frac{y}{\sigma_1}\sin\alpha + \frac{x^2 - y^2}{2\sigma_1^2}\cos 2\alpha + \frac{xy}{\sigma_1^2}\sin 2\alpha]$$

$$\cdot [F_{+s}\cos(\omega_{01} t - p\alpha) + F_{-s}\cos(\omega_{01} t + p\alpha) \tag{4}$$

$$+ F_{+r}\cos(\beta_1 + s_1\omega_{01} t - p\alpha - \varphi_{10}) + F_{-r}\cos(\beta_1 + s_1\omega_{01} t + p\alpha - \varphi_{20})]^2\} d(p\alpha),$$

where R_{01} is the inner radius of the controllable motor stator, l_{01} is the effective length of the rotor, $\Lambda_{01} = \mu_0 / \sigma_1$ is the even air-gap permeance of the controllable motor, μ_0 is the magnetic permeability coefficient of air, $\sigma_1 = k_{\mu 1}\delta_{01}$, k_μ is saturation, δ_{01} is the uniform air-gap size, $k_{\mu 1} = 1 + \delta_{F_e} / k_1\delta_{01}$, k_1 is the calculation air-gap coefficient of the even air-gap, δ_{F_e} is the equivalent air-gap of ferromagnetic materials, φ_{10} is the phase angle of the positive-sequence current of rotor lagging behind the positive-sequence current of stator, φ_{20} is the phase angle of the negative-sequence current of rotor lagging behind the negative-sequence current of stator. p is the number of the magnetic pole-pairs of compounded magnetic field of the motor. F_{+s}, F_{-s}, F_{+r} and F_{-r} are the positive-sequence and negative-sequence components of the magnetomotive amplitude of stator and rotor respectively (see the Appendix).

Substituting Eq. (3) into Eq. (4), rearranging, the following equation can be obtained as:

$$\begin{cases} V_{12} = (1 + \dfrac{x^2 + y^2}{2})\mathrm{g}_1 + \dfrac{x^2 - y^2}{2}\mathrm{g}_2 + xy\mathrm{g}_3, & (p = 1) \\ V_{12} = (1 + \dfrac{x^2 + y^2}{2})\mathrm{g}_1, & (p \neq 1) \end{cases} \tag{5}$$

where:

$$\begin{cases} g_1 = \dfrac{\pi p R_{01} l_{01} \Lambda_{01}}{4\sigma_1^2}\{F_{+s}^2 + F_{-s}^2 + F_{+r}^2 + F_{-r}^2 + 2F_{+s}F_{-s}\cos 2\omega_{01}t + 2F_{+s}F_{+r}\cos\varphi_{10} + 2F_{+s}F_{-r}\cos[\beta_1 \\ \quad + (1+s_1)\omega_{01}t - \varphi_{20}] + 2F_{-s}F_{+r}\cos[\beta_1 + (1+s_1)\omega_{01}t - \varphi_{10}] + 2F_{-s}F_{-r}\cos\varphi_{20} \\ \quad + 2F_{+r}F_{-r}\cos(2\beta_1 + 2s_1\omega_{01}t - \varphi_{10} - \varphi_{20})\} \\ g_2 = \dfrac{\pi p R_{01} l_{01} \Lambda_{01}}{2}\{\dfrac{1}{2}F_{+s}^2\cos 2\omega_{01}t + \dfrac{1}{2}F_{-s}^2\cos 2\omega_{01}t + \dfrac{1}{2}F_{+r}^2\cos(2\beta_1 + 2s_1\omega_{01}t - 2\varphi_{10}) \\ \quad + \dfrac{1}{2}F_{-r}^2\cos(2\beta_1 + 2s_1\omega_{01}t - 2\varphi_{20}) + F_{+s}F_{-s} + F_{+s}F_{+r}\cos[\beta_1 + (1+s_1)\omega_{01}t - \varphi_{10}] \\ \quad + F_{+s}F_{-r}\cos(-\varphi_{20}) + F_{-s}F_{+r}\cos(-\varphi_{10}) + F_{-s}F_{-r}\cos[\beta_1 + (1+s_1)\omega_{01}t - \varphi_{20}] \\ \quad + F_{+r}F_{-r}\cos(\varphi_{10} - \varphi_{20})\} \\ g_3 = \dfrac{\pi p R_{01} l_{01} \Lambda_{01}}{2}\{\dfrac{1}{2}F_{+s}^2\sin 2\omega_{01}t - \dfrac{1}{2}F_{-s}^2\sin 2\omega_{01}t + \dfrac{1}{2}F_{+r}^2\sin(2\beta_1 + 2s_1\omega_{01}t - 2\varphi_{10}) \\ \quad - \dfrac{1}{2}F_{-r}^2\sin(2\beta_1 + 2s_1\omega_{01}t - 2\varphi_{20}) + F_{+s}F_{+r}\sin[\beta_1 + (1+s_1)\omega_{01}t - \varphi_{10}] - F_{+s}F_{-r}\sin(-\varphi_{20}) \\ \quad - F_{-s}F_{+r}\sin(-\varphi_{10}) - F_{-s}F_{-r}\sin[\beta_1 + (1+s_1)\omega_{01}t - \varphi_{20}] - F_{+r}F_{-r}\sin(\varphi_{10} - \varphi_{20})\} \end{cases} \tag{6}$$

and the electromagnetic torque of the controllable motor can be expressed as:

$$T_{e1} = \frac{\partial V_{12}}{\partial \beta_1} \tag{7}$$

Substituting Eq. (5) into Eq. (7):

$$\begin{cases} T_{e1} = \varepsilon_{01}(U_1 + e_{11})(-g_1\sin\beta_1 - g_2\sin\beta_1 + g_3\cos\beta_1) \\ \quad + \varepsilon_{01}(U_2 + e_{12})(g_1\cos\beta_1 - g_2\cos\beta_1 - g_3\sin\beta_1) \\ \quad + \varepsilon_{01}^2(g_3\cos 2\beta_1 - g_2\sin 2\beta_1) + \dot{g}_1 + \dfrac{(U_1 + e_{11} + \varepsilon_{01}\cos\beta_1)^2}{2}(\dot{g}_1 + \dot{g}_2) \\ \quad + \dfrac{(U_2 + e_{12} + \varepsilon_{01}\sin\beta_1)^2}{2}(\dot{g}_1 - \dot{g}_2) + [-\varepsilon_{01}(U_2 + e_{12} + \varepsilon_{01}\sin\beta_1)\sin\beta_1 \\ \quad + \varepsilon_{01}(U_1 + e_{11} + \varepsilon_{01}\cos\beta_1)\cos\beta_1]g_3 \\ \quad + [(U_1 + e_{11} + \varepsilon_{01}\cos\beta_1)(U_2 + e_{12} + \varepsilon_{01}\sin\beta_1)]\dot{g}_3, \qquad (p = 1) \\ T_{e1} = [-\varepsilon_{01}(U_1 + e_{11})\sin\beta_1 + (U_2 + e_{12})\cos\beta_1]g_1 \\ \quad + [1 + \dfrac{(U_1 + e_{11} + \varepsilon_{01}\cos\beta_1)^2 + (U_2 + e_{12} + \varepsilon_{01}\sin\beta_1)^2}{2}]\dot{g}_1, \qquad (p \neq 1) \end{cases} \tag{8}$$

In the real working conditions, the rotational speed of the controllable motors will significantly decrease, generally. In that moment, the motors operate in the nonlinear area. The

characteristics are that the slide ratio s is greater than the critical slide ratio s_c. Therefore, during speed regulation, the condition of the controllable motors working in nonlinear areas is mainly studied.

As far as the controllable motor, the dynamic equation of the rotor can be expressed as:

$$J_{01}\frac{d^2\beta_1}{dt^2} = T_{e1} - T_{L1} - T_{R1} \tag{9}$$

where β_1 is the rotation angle of the motor shaft, J_{01} is the moment of inertia of the rotor, T_{e1} is electromagnetic torque, T_{L1} is the load torque, namely, the force that the close-chain linkage mechanism apply on the motor shaft. T_{R1} is the moment of resistance of the mechanical dissipation, including copper loss, iron loss, mechanical loss and additional mechanical loss of the armature.

$$T_{L1} = \frac{G_1 I_{P1}}{l_0} U_4 \tag{10}$$

where G_1 is the shear modulus of the materials of controllable motor 1 shaft, I_{P1} is the moment of inertia distribution function of the rotor, and l_0 is the length of the output shaft of the servomotor.

Generally, T_{R1} only reach 3 %-5 % of the electromagnetic torque T_{e1}, and T_{R1} can be neglected. Therefore, Eq. (8) can be expressed as:

$$J_{01}\ddot{\beta}_1 = T_{e1} - T_{L1}. \tag{11}$$

The condition $p = 1$ is considered in this paper, and substituting Eq. (8) into Eq. (11), rearranging, and it is gained:

$$\begin{aligned}
\ddot{\beta}_1 = {} & \frac{\varepsilon_{01}(U_1 + e_{11})}{J_{01}}(-\mathrm{g}_1 \sin\beta_1 - \mathrm{g}_2 \sin\beta_1 + \mathrm{g}_3 \cos\beta_1) + \frac{\varepsilon_{01}(U_2 + e_{12})}{J_{01}}(\mathrm{g}_1 \cos\beta_1 \\
& - \mathrm{g}_2 \cos\beta_1 - \mathrm{g}_3 \sin\beta_1) + \frac{\varepsilon_{01}^2}{J_{01}}(\mathrm{g}_3 \cos 2\beta_1 - \mathrm{g}_2 \sin 2\beta_1) + \frac{\dot{\mathrm{g}}_1}{J_{01}} \\
& + \frac{(U_1 + e_{11} + \varepsilon_{01}\cos\beta_1)^2}{2J_{01}}(\dot{\mathrm{g}}_1 + \dot{\mathrm{g}}_2) + \frac{(U_2 + e_{12} + \varepsilon_{01}\sin\beta_1)^2}{2J_{01}}(\dot{\mathrm{g}}_1 - \dot{\mathrm{g}}_2) \\
& + \frac{1}{J_{01}}[-\varepsilon_{01}(U_2 + e_{12} + \varepsilon_{01}\sin\beta_1)\sin\beta_1 + \varepsilon_{01}(U_1 + e_{11} + \varepsilon_{01}\cos\beta_1)\cos\beta_1]\mathrm{g}_3 \\
& + \frac{1}{J_{01}}[(U_1 + e_{11} + \varepsilon_{01}\cos\beta_1)(U_2 + e_{12} + \varepsilon_{01}\sin\beta_1)]\dot{\mathrm{g}}_3 - \frac{G_1 I_{P1}}{J_{01} l_0} U_4.
\end{aligned} \tag{12}$$

Similarly, for the 3-phase AC motor:

$$\begin{aligned}
\ddot{\beta}_4 = {} & \frac{\varepsilon_{02}(U_5 + e_{21})}{J_{02}}(-h_1 \sin\beta_4 - h_2 \sin\beta_4 + h_3 \cos\beta_4) \\
& + \frac{\varepsilon_{02}(U_6 + e_{22})}{J_{02}}(h_1 \cos\beta_4 - h_2 \cos\beta_4 - h_3 \sin\beta_4) \\
& + \frac{\varepsilon_{02}^2}{J_{02}}(h_3 \cos 2\beta_4 - h_2 \sin 2\beta_4) + \frac{\dot{h}_1}{J_{02}} + \frac{(U_5 + e_{21} + \varepsilon_{02}\cos\beta_4)^2}{2J_{02}}(\dot{h}_1 + \dot{h}_2) \\
& + \frac{(U_2 + e_{22} + \varepsilon_{02}\sin\beta_4)^2}{2J_{02}}(\dot{h}_1 - \dot{h}_2) + \frac{1}{J_{02}}[-\varepsilon_{02}(U_6 + e_{22} + \varepsilon_{02}\sin\beta_4)\sin\beta_4
\end{aligned}$$

$$+\varepsilon_{02}(U_1+e_{21}+\varepsilon_{02}\cos\beta_4)\cos\beta_4]h_3$$
$$+\frac{1}{J_{02}}[(U_1+e_{21}+\varepsilon_{02}\cos\beta_4)(U_6+e_{22}+\varepsilon_{02}\sin\beta_4)]\dot{h}_3-\frac{G_2I_{P2}}{J_{02}l_0'}U_8, \tag{13}$$

$$\begin{cases} h_1=\dfrac{\pi R_{02}l_{02}\Lambda_{02}}{2}[F_{1m}^2+F_{2m}^2+2F_{1m}F_{2m}\cos\phi] \\ h_2=\dfrac{\pi R_{02}l_{02}\Lambda_{02}}{4}[F_{1m}^2\cos(2\omega_{02}t)+F_{2m}^2\cos(2\omega_{02}t-2\phi)+2F_{1m}F_{2m}\cos(2\omega_{02}t-\phi)] \\ h_3=\dfrac{\pi R_{02}l_{02}\Lambda_{02}}{4}[F_{1m}^2\sin(2\omega_{02}t)+F_{2m}^2\sin(2\omega_{02}t-2\phi)+2F_{1m}F_{2m}\sin(2\omega_{02}t-\phi)] \end{cases} \tag{14}$$

where G_2 is the shear modulus of the material of the 3-phase AC motor shaft, I_{P2} is the polar inertia moment of cross-section of the 3-phase AC motor shaft. l_0' is the length of the output shaft of the 3-phase AC motor. R_{02} is the inner radius of the 3-phase AC motor stator, l_{02} is the effective length of the rotor, $\Lambda_{02}=\mu_0/\sigma_2$ is the even air-gap permeance of the 3-phase AC motor, μ_0 is the magnetic permeability coefficient of air, $\sigma_2=k_{\mu 2}\delta_{02}$, $k_{\mu 2}$ is saturation, δ_{02} is the uniform air-gap size, $k_{\mu 2}=1+\delta_{F_e}/k_2\delta_{02}$, k_2 is the calculation air-gap coefficient of the even air gap of the 3-phase AC motor, δ_{F_e} is the equivalent air-gap of ferromagnetic materials, ω_{02} is the synchronous speed of the 3-phase AC motor, ϕ is the phase angle of the positive-sequence current of rotor lagging behind the positive-sequence current of stator of the 3-phase AC motor, F_{1m} and F_{2m} are the magnetomotive amplitude of stator and rotor of the 3-phase AC motor, respectively.

Replacing elastic displacement U_i in Eqs. (12) and (13) by generalized coordinate $\boldsymbol{u}$:

$$\begin{aligned}\ddot{\beta}_1=&\boldsymbol{k}_{e1}\boldsymbol{u}+\boldsymbol{u}^T\boldsymbol{k}_{e2}\boldsymbol{u}+\frac{\varepsilon_{01}e_{11}}{J_{01}}(-\mathrm{g}_1\sin\beta_1-\mathrm{g}_2\sin\beta_1+\mathrm{g}_3\cos\beta_1)\\&+\frac{\varepsilon_{01}e_{12}}{J_{01}}(\mathrm{g}_1\cos\beta_1-\mathrm{g}_2\cos\beta_1-\mathrm{g}_3\sin\beta_1)+\frac{\varepsilon_{01}^2}{J_{01}}(\mathrm{g}_3\cos 2\beta_1-\mathrm{g}_2\sin 2\beta_1)\\&+\frac{\mathrm{g}_1'}{J_{01}}+\frac{(e_{11}+\varepsilon_{01}\cos\beta_1)^2}{2J_{01}}(\mathrm{g}_1'+\mathrm{g}_2')+\frac{(e_{12}+\varepsilon_{01}\sin\beta_1)^2}{2J_{01}}(\mathrm{g}_1'-\mathrm{g}_2')\\&+\frac{1}{J_{01}}[-\varepsilon_{01}(e_{12}+\varepsilon_{01}\sin\beta_1)\sin\beta_1+\varepsilon_{01}(e_{11}+\varepsilon_{01}\cos\beta_1)\cos\beta_1]\mathrm{g}_3\\&+\frac{1}{J_{01}}(e_{11}+\varepsilon_{01}\cos\beta_1)(e_{12}+\varepsilon_{01}\sin\beta_1)\mathrm{g}_3'.\end{aligned} \tag{15}$$

$$\begin{aligned}\ddot{\beta}_4=&\boldsymbol{k}_{\varepsilon 1}\boldsymbol{u}+\boldsymbol{u}^T\boldsymbol{k}_{\varepsilon 2}\boldsymbol{u}+\frac{\varepsilon_{02}e_{21}}{J_{02}}(-h_1\sin\beta_4-h_2\sin\beta_4+h_3\cos\beta_4)\\&+\frac{\varepsilon_{02}e_{22}}{J_{02}}(h_1\cos\beta_4-h_2\cos\beta_4-h_3\sin\beta_4)+\frac{\varepsilon_{02}^2}{J_{02}}(h_3\cos 2\beta_4-h_2\sin 2\beta_4)\\&+\frac{h_1'}{J_{02}}+\frac{(e_{21}+\varepsilon_{02}\cos\beta_4)^2}{2J_{02}}(h_1'+h_2')+\frac{(e_{22}+\varepsilon_{02}\sin\beta_4)^2}{2J_{02}}(h_1'-h_2')\\&+\frac{1}{J_{02}}[-\varepsilon_{02}(e_{22}+\varepsilon_{02}\sin\beta_4)\sin\beta_4+\varepsilon_{02}(e_{21}+\varepsilon_{02}\cos\beta_4)\cos\beta_4]h_3\end{aligned}$$

$$+\frac{1}{J_{02}}(e_{21}+\varepsilon_{02}\cos\beta_4)(e_{22}+\varepsilon_{02}\sin\beta_4)h_3', \tag{16}$$

where $\boldsymbol{k}_{e1}$, $\boldsymbol{k}_{\varepsilon 1}$ and $\boldsymbol{k}_{e2}$ are all the nth-order vector, and:

$$(\boldsymbol{k}_{e1})_1=\frac{\varepsilon_{01}}{J_{01}}(-\mathrm{g}_1\sin\beta_1-\mathrm{g}_2\sin\beta_1+\mathrm{g}_3\cos\beta_1),\ (\boldsymbol{k}_{e1})_2=\frac{\varepsilon_{01}}{J_{01}}(\mathrm{g}_1\cos\beta_1-\mathrm{g}_2\cos\beta_1-\mathrm{g}_3\sin\beta_1),$$

$$(\boldsymbol{k}_{e1})_4=-\frac{G_1I_{P1}}{J_{01}l_0},\ (\boldsymbol{k}_{\varepsilon 1})_1=-\frac{\mathrm{g}_1\varepsilon_{01}}{J_{01}}\sin\beta_1,\ (\boldsymbol{k}_{\varepsilon 1})_2=\frac{\mathrm{g}_1}{J_{01}}\cos\beta_1,\ (\boldsymbol{k}_{\varepsilon 1})_4=-\frac{G_1I_{P1}}{J_{01}l_0},$$

$$(\boldsymbol{k}_{e2})_5=\frac{\varepsilon_{02}}{J_{02}}(-h_1\sin\beta_4-h_2\sin\beta_4+h_3\cos\beta_4),\ (\boldsymbol{k}_{e2})_8=-\frac{G_2I_{P2}}{J_{02}l_0'},\ (\boldsymbol{k}_{\varepsilon 2})_{55}=\frac{h_1'+h_2'}{2J_{02}},$$

$$(\boldsymbol{k}_{e2})_6=\frac{\varepsilon_{02}}{J_{02}}(h_1\cos\beta_4-h_2\cos\beta_4-h_3\sin\beta_4),\ (\boldsymbol{k}_{\varepsilon 2})_{66}=\frac{h_1'-h_2'}{2J_{02}},\ (\boldsymbol{k}_{\varepsilon 2})_{56}=(\boldsymbol{k}_{\varepsilon 2})_{65}=\frac{h_3'}{2J_{02}},$$

and the other terms of the $\boldsymbol{k}_{e1}$, $\boldsymbol{k}_{\varepsilon 1}$, $\boldsymbol{k}_{e2}$ and $\boldsymbol{k}_{\varepsilon 2}$ are all zero.

$\ddot{\boldsymbol{u}}_r$ is the rigid acceleration array of the system in the global coordinates, and can be expressed as:

$$\ddot{\boldsymbol{u}}_r=\boldsymbol{u}_{\omega 1}\dot{\beta}_1^2+\boldsymbol{u}_{\omega 2}\dot{\beta}_4^2+\boldsymbol{u}_{\omega 3}\dot{\beta}_1\dot{\beta}_4+\boldsymbol{u}_{\varepsilon 1}\ddot{\beta}_1+\boldsymbol{u}_{\varepsilon 2}\ddot{\beta}_4 \tag{17}$$

where $\boldsymbol{u}_{\omega 1}$, $\boldsymbol{u}_{\omega 2}$, $\boldsymbol{u}_{\omega 3}$, $\boldsymbol{u}_{\varepsilon 1}$ and $\boldsymbol{u}_{\varepsilon 2}$ are coefficient arrays in connection with geometric dimensions and position of linkage mechanism, and can be obtained from rigid kinematics analysis of linkage mechanism system. Then, the self-excited inertia force of the system can be expressed as:

$$\boldsymbol{Q}=-\boldsymbol{M}(\boldsymbol{u}_{\omega 1}\dot{\beta}_1^2+\boldsymbol{u}_{\omega 2}\dot{\beta}_4^2+\boldsymbol{u}_{\omega 3}\dot{\beta}_1\dot{\beta}_4+\boldsymbol{u}_{\varepsilon 1}\ddot{\beta}_1+\boldsymbol{u}_{\varepsilon 2}\ddot{\beta}_4). \tag{18}$$

Because $-\boldsymbol{M}(\boldsymbol{u}_{\varepsilon 1}\ddot{\beta}_1+\boldsymbol{u}_{\varepsilon 2}\ddot{\beta}_4)$ is small, the Eq. (17) can be expressed as:

$$\boldsymbol{Q}=-\boldsymbol{M}(\boldsymbol{u}_{\omega 1}\dot{\beta}_1^2+\boldsymbol{u}_{\omega 2}\dot{\beta}_4^2+\boldsymbol{u}_{\omega 3}\dot{\beta}_1\dot{\beta}_4)-\varepsilon\boldsymbol{M}(\boldsymbol{u}_{\varepsilon 1}\ddot{\beta}_1+\boldsymbol{u}_{\varepsilon 2}\ddot{\beta}_4) \tag{19}$$

where ε expressed as a small parameter. When working of the close-chain linkage mechanism, the instantaneous angular velocity $\dot{\beta}_4$ of the 3-phase AC motor rotator is a periodic function. And when working under given trajectory in linkage workspace, $\dot{\beta}_1$ also is a periodic function. Therefore $-\boldsymbol{M}(\boldsymbol{u}_{\omega 1}\dot{\beta}_1^2+\boldsymbol{u}_{\omega 2}\dot{\beta}_4^2+\boldsymbol{u}_{\omega 3}\dot{\beta}_1\dot{\beta}_4)$ is a periodic function, given as:

$$-\boldsymbol{M}(\boldsymbol{u}_{\omega 1}\dot{\beta}_1^2+\boldsymbol{u}_{\omega 2}\dot{\beta}_4^2+\boldsymbol{u}_{\omega 3}\dot{\beta}_1\dot{\beta}_4)=\boldsymbol{F}_1+\boldsymbol{F}_2+\boldsymbol{F}_3 \tag{20}$$

where $\boldsymbol{F}_1$, $\boldsymbol{F}_2$ and $\boldsymbol{F}_3$ are vectors of the k-order term of the expansion of the Fourier series, and:

$$\begin{cases}(\boldsymbol{F}_1)_i=\sum_{k=1}^{m}F_{1ki}\cos(kv_1t+\tau_{1ki})\\(\boldsymbol{F}_2)_i=\sum_{k=1}^{m}F_{2ki}\cos(kv_2t+\tau_{2ki})\\(\boldsymbol{F}_3)_i=\sum_{k=1}^{m}F_{3ki}\cos(kv_3t+\tau_{3ki})\end{cases} \tag{21}$$

where v_1 is the working frequency of rotor of controllable motor 1, v_2 is the working frequency of rotor of controllable motor 2, v_3 is the smallest common multiple of v_1 and v_2. F_{1ki}, F_{2ki} and F_{3ki} express the amplitude values, and τ_{1ki}, τ_{2ki} and τ_{3ki} are the corresponding phase angles, and m is the number of terms of the Fourier expansion formula.

Substituting Eqs. (15), (16) and (20) into Eq. (19), under the condition $p=1$, the self-excitation inertia of the system is obtained:

$$\boldsymbol{Q}=\boldsymbol{F}_1+\boldsymbol{F}_2+\boldsymbol{F}_3-\varepsilon(\boldsymbol{M}\boldsymbol{u}_{\varepsilon 1}\boldsymbol{k}_{e1}\boldsymbol{u}+\boldsymbol{M}\boldsymbol{u}_{\varepsilon 1}\boldsymbol{u}^T\boldsymbol{k}_{e2}\boldsymbol{u}+\lambda_1\boldsymbol{M}\boldsymbol{u}_{\varepsilon 1}+\boldsymbol{M}\boldsymbol{u}_{\varepsilon 2}\boldsymbol{k}_{\varepsilon 1}\boldsymbol{u}+\boldsymbol{M}\boldsymbol{u}_{\varepsilon 2}\boldsymbol{u}^T\boldsymbol{k}_{\varepsilon 2}\boldsymbol{u}+\lambda_2\boldsymbol{M}\boldsymbol{u}_{\varepsilon 2}) \tag{22}$$

where:

$$\begin{aligned}\lambda_1=&\frac{\varepsilon_{01}e_{11}}{J_{01}}(-\mathrm{g}_1\sin\beta_1-\mathrm{g}_2\sin\beta_1+\mathrm{g}_3\cos\beta_1)+\frac{\varepsilon_{01}e_{12}}{J_{01}}(\mathrm{g}_1\cos\beta_1-\mathrm{g}_2\cos\beta_1-\mathrm{g}_3\sin\beta_1)\\&+\frac{\varepsilon_{01}^2}{J_{01}}(\mathrm{g}_3\cos 2\beta_1-\mathrm{g}_2\sin 2\beta_1)+\frac{\mathrm{g}_1'}{J_{01}}+\frac{(e_{11}+\varepsilon_{01}\cos\beta_1)^2}{2J_{01}}(\mathrm{g}_1'+\mathrm{g}_2')\\&+\frac{(e_{12}+\varepsilon_{01}\sin\beta_1)^2}{2J_{01}}(\mathrm{g}_1'-\mathrm{g}_2')+\frac{1}{J_{01}}[-\varepsilon_{01}(e_{12}+\varepsilon_{01}\sin\beta_1)\sin\beta_1\\&+\varepsilon_{01}(e_{11}+\varepsilon_{01}\cos\beta_1)\cos\beta_1]\mathrm{g}_3+\frac{1}{J_{01}}(e_{11}+\varepsilon_{01}\cos\beta_1)(e_{12}+\varepsilon_{01}\sin\beta_1)\mathrm{g}_3'\end{aligned} \tag{23}$$

$$\begin{aligned}\lambda_2=&\frac{\varepsilon_{02}e_{21}}{J_{02}}(-h_1\sin\beta_4-h_2\sin\beta_4+h_3\cos\beta_4)\\&+\frac{\varepsilon_{02}e_{22}}{J_{02}}(h_1\cos\beta_4-h_2\cos\beta_4-h_3\sin\beta_4)+\frac{\varepsilon_{02}^2}{J_{02}}(h_3\cos 2\beta_4-h_2\sin 2\beta_4)\\&+\frac{h_1'}{J_{02}}+\frac{(e_{21}+\varepsilon_{02}\cos\beta_4)^2}{2J_{02}}(h_1'+h_2')+\frac{(e_{22}+\varepsilon_{02}\sin\beta_4)^2}{2J_{02}}(h_1'-h_2')\\&+\frac{1}{J_{02}}[-\varepsilon_{02}(e_{22}+\varepsilon_{02}\sin\beta_4)\sin\beta_4+\varepsilon_{02}(e_{21}+\varepsilon_{02}\cos\beta_4)\cos\beta_4]h_3\\&+\frac{1}{J_{02}}(e_{21}+\varepsilon_{02}\cos\beta_4)(e_{22}+\varepsilon_{02}\sin\beta_4)h_3'\end{aligned} \tag{24}$$

and assumes that:

$$-(\boldsymbol{K}_{11}^e+\boldsymbol{K}_{12}^e+\boldsymbol{K}_{21}^e+\boldsymbol{K}_{22}^e)\boldsymbol{e}-\boldsymbol{k}_0=\boldsymbol{F}_4+\boldsymbol{F}_5+\boldsymbol{F}_6+\boldsymbol{F}_7+\boldsymbol{F}_8. \tag{25}$$

According to [8]:

$$\begin{cases}\boldsymbol{F}_4=[a_1,a_2,\cdots,a_n]^T\\ \boldsymbol{F}_5=[b_1,b_2,\cdots,b_n]^T\\ \boldsymbol{F}_6=[c_1,c_2,\cdots,c_n]^T\\ \boldsymbol{F}_7=[d_1,d_2,\cdots,d_n]^T\\ \boldsymbol{F}_8=[f_1,f_2,\cdots,f_n]^T\end{cases} \tag{26}$$

where:

$$a_1 = -[(\bar{\boldsymbol{K}}_{\mathbf{11}})_{11} + (\bar{\boldsymbol{K}}_{\mathbf{21}})_{11}](e_{11} + e_{21} + \varepsilon_{01}\cos\beta_1) - (\bar{\boldsymbol{K}}_{\mathbf{11}})_{12}(e_{12} + e_{22} + \varepsilon_{01}\sin\beta_1),$$

$$a_2 = -(\bar{\boldsymbol{K}}_{\mathbf{11}})_{21}(e_{11} + e_{21} + \varepsilon_{01}\cos\beta_1) - [(\bar{\boldsymbol{K}}_{\mathbf{11}})_{22} + (\bar{\boldsymbol{K}}_{\mathbf{21}})_{22}](e_{12} + e_{22} + \varepsilon_{01}\sin\beta_1),$$

$$b_1 = -[(\bar{\boldsymbol{K}}_{\mathbf{12}})_{11} + (\bar{\boldsymbol{K}}_{\mathbf{21}})_{11}](\varepsilon_{02}\cos\beta_4) - (\bar{\boldsymbol{K}}_{\mathbf{12}})_{12}(\varepsilon_{02}\sin\beta_4),$$

$$b_2 = -(\bar{\boldsymbol{K}}_{\mathbf{12}})_{21}(\varepsilon_{02}\cos\beta_4) - [(\bar{\boldsymbol{K}}_{\mathbf{12}})_{22} + (\bar{\boldsymbol{K}}_{\mathbf{21}})_{22}](\varepsilon_{02}\sin\beta_4),$$

$$c_1 = -(\bar{\boldsymbol{K}}_{\mathbf{12}})_{11}e_{11} - (\bar{\boldsymbol{K}}_{\mathbf{12}})_{12}e_{12} - (\bar{\boldsymbol{k}}_{01})_1,\ c_2 = -(\bar{\boldsymbol{K}}_{\mathbf{12}})_{21}e_{11} - [(\bar{\boldsymbol{K}}_{\mathbf{12}})_{22} + (\bar{\boldsymbol{K}}_{\mathbf{22}})_{22}e_{12} + (\bar{\boldsymbol{k}}_{01})_2,$$

$$d_1 = -(\bar{\boldsymbol{K}}_{\mathbf{22}})_{11}e_{11} - (\bar{\boldsymbol{K}}_{\mathbf{22}})_{12}e_{12} - (\bar{\boldsymbol{k}}_{02})_1,\ d_2 = -(\boldsymbol{K}_{\mathbf{22}})_{21}e_{11} - (\bar{\boldsymbol{K}}_{\mathbf{22}})_{22}e_{12} - (\bar{\boldsymbol{k}}_{02})_2,$$

$$\begin{aligned} f_1 = &-[(\bar{\boldsymbol{K}}_{\mathbf{12}})_{11} + (\bar{\boldsymbol{K}}_{\mathbf{22}})_{11}](\varepsilon_{01}\cos\beta_1 + e_{21} + \varepsilon_{02}\cos\beta_4) \\ &-[(\bar{\boldsymbol{K}}_{\mathbf{12}})_{12} + (\bar{\boldsymbol{K}}_{\mathbf{22}})_{12}](\varepsilon_{01}\sin\beta_1 + e_{22} + \varepsilon_{02}\sin\beta_4), \\ f_2 = &-[(\bar{\boldsymbol{K}}_{\mathbf{12}})_{21} + (\boldsymbol{K}_{\mathbf{22}})_{21}](\varepsilon_{01}\cos\beta_1 + e_{21} + \varepsilon_{02}\cos\beta_4) \\ &-[(\bar{\boldsymbol{K}}_{\mathbf{12}})_{22} + (\bar{\boldsymbol{K}}_{\mathbf{22}})_{22}](\varepsilon_{01}\sin\beta_1 + e_{22} + \varepsilon_{02}\sin\beta_4), \end{aligned}$$

and the other components of $\boldsymbol{F}_4$, $\boldsymbol{F}_5$, $\boldsymbol{F}_6$, $\boldsymbol{F}_7$ and $\boldsymbol{F}_8$ are equal to zero.

Therefore $\boldsymbol{F}_4$, $\boldsymbol{F}_5$, $\boldsymbol{F}_6$, $\boldsymbol{F}_7$ and $\boldsymbol{F}_8$ are periodic functions. They can be expanded in the form of Fourier series as follows:

$$\begin{cases} (\boldsymbol{F}_4)_i = \sum_{k=1}^{m} F_{4ki}\cos(kv_4 t + \tau_{4ki}) \\ (\boldsymbol{F}_5)_i = \sum_{k=1}^{m} F_{5ki}\cos(kv_5 t + \tau_{5ki}) \\ (\boldsymbol{F}_6)_i = \sum_{k=1}^{m} F_{6ki}\cos(kv_6 t + \tau_{6ki}) \\ (\boldsymbol{F}_7)_i = \sum_{k=1}^{m} F_{7ki}\cos(kv_7 t + \tau_{7ki}) \\ (\boldsymbol{F}_8)_i = \sum_{k=1}^{m} F_{8ki}\cos(kv_8 t + \tau_{8ki}) \end{cases} \tag{27}$$

where $v_4 = v_1$, $v_5 = v_2$, v_6 is the rotation frequency of magnetic field of stator of the controllable motor 1, v_7 is the rotation frequency of magnetic field of stator of the controllable motor 2, v_5 is the smallest common multiple of v_6 and v_7, and v_8 is the smallest common multiple of v_1, v_2, v_6 and v_7. F_{4ki}, F_{5ki}, F_{6ki}, F_{7ki} and F_{8ki} express the amplitude values, and τ_{4ki}, τ_{5ki}, τ_{6ki}, τ_{7ki} and τ_{8ki} are the corresponding phase angles, and m is the number of terms of the Fourier expansion formula.

Substituting Eqs. (21) and (27) into Eq. (1):

$$\begin{aligned} &\boldsymbol{M}\ddot{\boldsymbol{u}} + \boldsymbol{C}\dot{\boldsymbol{u}} + (\boldsymbol{K} + \boldsymbol{K}_0)\boldsymbol{u} = \boldsymbol{P} + \sum_{f=1}^{8}\boldsymbol{F}_f \\ &+\varepsilon[-\boldsymbol{M}\boldsymbol{u}_{\varepsilon 1}\boldsymbol{k}_{e1}\boldsymbol{u} - \boldsymbol{M}\boldsymbol{u}_{\varepsilon 1}\boldsymbol{u}^T\boldsymbol{k}_{e2}\boldsymbol{u} - \lambda_1\boldsymbol{M}\boldsymbol{u}_{\varepsilon 1} - \boldsymbol{M}\boldsymbol{u}_{\varepsilon 2}\boldsymbol{k}_{\varepsilon 1}\boldsymbol{u} - \boldsymbol{M}\boldsymbol{u}_{\varepsilon 2}\boldsymbol{u}^T\boldsymbol{k}_{\varepsilon 2}\boldsymbol{u} - \lambda_2\boldsymbol{M}\boldsymbol{u}_{\varepsilon 2} \\ &+\sum_{n=1}^{8}\boldsymbol{u}^{\mathrm{T}}\boldsymbol{G}_n\boldsymbol{K}_n\boldsymbol{u} + \frac{1}{2}\sum_{n=1}^{8}\boldsymbol{u}^{\mathrm{T}}\boldsymbol{K}_n\boldsymbol{u}\boldsymbol{G}_n + \frac{1}{2}\sum_g\sum_l\boldsymbol{u}^{\mathrm{T}}\boldsymbol{G}_{gl}\boldsymbol{u}\boldsymbol{K}_{gl}\boldsymbol{u} + \frac{1}{2}\sum_g\sum_l\boldsymbol{G}_{gl}\boldsymbol{u}\boldsymbol{u}^{\mathrm{T}}\boldsymbol{K}_{gl}\boldsymbol{u}], \\ &(g,\ l = 2,\ 3,\ 4,\ 6,\ 7,\ 8). \end{aligned} \tag{28}$$

Decoupling the dynamic model of the system

Assuming that the linear transfer functions are:

$$\boldsymbol{u} = \boldsymbol{\phi}\boldsymbol{\eta} \tag{29}$$

where $\boldsymbol{\phi}$ is the modal transfer matrix, $\boldsymbol{\eta}$ is the modal coordinate vector. Substituting Eq. (29) into Eq. (28), and pre-multiplying the equation by $\boldsymbol{\phi}^{\mathrm{T}}$, then the Eq. (28) can be represented as:

$$\begin{aligned}\ddot{\boldsymbol{\eta}} + \boldsymbol{\omega}^2\boldsymbol{\eta} = \boldsymbol{P}_0 + \sum_{f=1}^{8}\boldsymbol{F}_{0f} + \varepsilon[&-\boldsymbol{K}_{00}\boldsymbol{\eta} - \boldsymbol{\phi}^T\boldsymbol{M}\boldsymbol{u}_{\varepsilon 1}\boldsymbol{k}_{e1}\boldsymbol{\phi}\boldsymbol{\eta} - \boldsymbol{\phi}^T\boldsymbol{M}\boldsymbol{u}_{\varepsilon 1}\boldsymbol{\phi}^T\boldsymbol{\eta}^T\boldsymbol{k}_{e2}\boldsymbol{\phi}\boldsymbol{\eta} - \lambda_1\boldsymbol{M}_0\boldsymbol{u}_{\varepsilon 1}\\ &-\boldsymbol{\phi}^T\boldsymbol{M}\boldsymbol{u}_{\varepsilon 2}\boldsymbol{k}_{\varepsilon 1}\boldsymbol{\phi}\boldsymbol{\eta} - \boldsymbol{\phi}^T\boldsymbol{M}\boldsymbol{u}_{\varepsilon 2}\boldsymbol{\phi}^T\boldsymbol{\eta}^T\boldsymbol{k}_{\varepsilon 2}\boldsymbol{\phi}\boldsymbol{\eta} - \lambda_2\boldsymbol{M}_0\boldsymbol{u}_{\varepsilon 2} + \sum_{n=1}^{8}\boldsymbol{\eta}^T\boldsymbol{G}_{0n}\boldsymbol{K}_{0n}\boldsymbol{\eta}\\ &+\frac{1}{2}\sum_{n=1}^{8}\boldsymbol{\eta}^T\boldsymbol{K}_{0n}\boldsymbol{\eta}\boldsymbol{G}_{0n} + \frac{1}{2}\sum_g\sum_l\boldsymbol{\eta}^T\boldsymbol{G}_{0gl}\boldsymbol{\eta}\boldsymbol{K}_{0gl}\boldsymbol{\eta} + \frac{1}{2}\sum_g\sum_l\boldsymbol{G}_{0gl}\boldsymbol{\eta}\boldsymbol{\eta}^T\boldsymbol{K}_{0gl}\boldsymbol{\eta} - \boldsymbol{C}_0\dot{\boldsymbol{\eta}}],\\ &(g,\ l = 2,\ 3,\ 4,\ 6,\ 7,\ 8)\end{aligned} \tag{30}$$

where:

$$\boldsymbol{\omega}^2 = \begin{bmatrix}\omega_1^2 & \cdots & 0\\ \vdots & \omega_2^2 & \vdots\\ & \ddots & \\ 0 & & \omega_n^2\end{bmatrix},\ \boldsymbol{C}_0 = \begin{bmatrix}2\zeta_1\omega_1 & \cdots & 0\\ \vdots & 2\zeta_2\omega_2 & \vdots\\ & \ddots & \\ 0 & & 2\zeta_n\omega_n\end{bmatrix},$$

$$\boldsymbol{P}_0 = \boldsymbol{\phi}^T\boldsymbol{P},\qquad \sum_{f=1}^{8}\boldsymbol{F}_{0f} = \sum_{f=1}^{8}\boldsymbol{\phi}^T\boldsymbol{F}_f,\qquad \boldsymbol{K}_{011}^e + \boldsymbol{K}_{012}^e + \boldsymbol{K}_{021}^e + \boldsymbol{K}_{022}^e = \boldsymbol{\phi}^T(\boldsymbol{K}_{11}^e + \boldsymbol{K}_{12}^e + \boldsymbol{K}_{21}^e + \boldsymbol{K}_{22}^e),$$

$$\boldsymbol{k}_{00} = \boldsymbol{\phi}^T\boldsymbol{k}_0,\quad \boldsymbol{K}_{00} = \boldsymbol{\phi}^T\boldsymbol{K}_0\boldsymbol{\phi},\quad \boldsymbol{G}_{0n} = \boldsymbol{\phi}^T\boldsymbol{G}_n,\quad \boldsymbol{M}_0 = \boldsymbol{\phi}^T\boldsymbol{M},\quad \boldsymbol{K}_{0n} = \boldsymbol{\phi}^T\boldsymbol{K}_n\boldsymbol{\phi},\quad \boldsymbol{G}_{0gl} = \boldsymbol{\phi}^T\boldsymbol{G}_{gl}\boldsymbol{\phi},$$

$\boldsymbol{K}_{0gl} = \boldsymbol{\phi}^{\mathrm{T}}\boldsymbol{K}_{gl}\boldsymbol{\phi}$. ζ_n and ω_n are the n-order damping ratio mean the n-order instantaneous natural frequency mean of the n-order canonical mode of the system in a period of motion, and ζ_n can be obtained through experiment.

Eq. (30) also can be expressed as:

$$\begin{aligned}\ddot{\eta}_r + \omega_r^2\eta_r = P_{0r} + \sum_{f=1}^{8}\boldsymbol{F}_{0fr}&\\ \varepsilon[&-2\zeta_r\omega_r\dot{\eta}_r - \boldsymbol{\xi}\boldsymbol{K}_{00}\boldsymbol{\eta} - \boldsymbol{\xi}\boldsymbol{\phi}^T\boldsymbol{M}\boldsymbol{u}_{\varepsilon 1}\boldsymbol{k}_{e1}\boldsymbol{\phi}\boldsymbol{\eta} - \boldsymbol{\xi}\boldsymbol{\phi}^T\boldsymbol{M}\boldsymbol{u}_{\varepsilon 1}\boldsymbol{\phi}^T\boldsymbol{\eta}^T\boldsymbol{k}_{e2}\boldsymbol{\phi}\boldsymbol{\eta} - \lambda_1\boldsymbol{\xi}\boldsymbol{M}_0\boldsymbol{u}_{\varepsilon 1}\\ &-\boldsymbol{\xi}\boldsymbol{\phi}^T\boldsymbol{M}\boldsymbol{u}_{\varepsilon 2}\boldsymbol{k}_{\varepsilon 1}\boldsymbol{\phi}\boldsymbol{\eta} - \boldsymbol{\xi}\boldsymbol{\phi}^T\boldsymbol{M}\boldsymbol{u}_{\varepsilon 2}\boldsymbol{\phi}^T\boldsymbol{\eta}^T\boldsymbol{k}_{\varepsilon 2}\boldsymbol{\phi}\boldsymbol{\eta} - \lambda_2\boldsymbol{\xi}\boldsymbol{M}_0\boldsymbol{u}_{\varepsilon 2} + \sum_{n=1}^{8}\boldsymbol{\xi}\boldsymbol{\eta}^T\boldsymbol{G}_{0n}\boldsymbol{K}_{0n}\boldsymbol{\eta}\\ &+\frac{1}{2}\sum_{n=1}^{8}\boldsymbol{\xi}\boldsymbol{\eta}^T\boldsymbol{K}_{0n}\boldsymbol{\eta}\boldsymbol{G}_{0n} + \frac{1}{2}\sum_g\sum_l\boldsymbol{\xi}\boldsymbol{\eta}^T\boldsymbol{G}_{0gl}\boldsymbol{\eta}\boldsymbol{K}_{0gl}\boldsymbol{\eta} + \frac{1}{2}\sum_g\sum_l\boldsymbol{\xi}\boldsymbol{G}_{0gl}\boldsymbol{\eta}\boldsymbol{\eta}^T\boldsymbol{K}_{0gl}\boldsymbol{\eta}],\\ &(g,\ l = 2,\ 3,\ 4,\ 6,\ 7,\ 8;\ r = 1,\ 2,\ \cdots,\ n)\end{aligned} \tag{31}$$

where $\boldsymbol{\xi}$ is the n-th order vector, and the r-th element of $\boldsymbol{\xi}$ is 1 and the other elements are zero, and n is the degree of freedom of system. Therefore, the system is affected by multifrequency excitations.

Eq. (31) also can be expressed as:

$$\ddot{\eta}_r + \omega_r^2 \eta_r = P_{0r} + \sum_{f=1}^{8} \boldsymbol{F}_{0fr} + \varepsilon(-2\zeta_r \omega_r \dot{\eta}_r - \lambda_1 \boldsymbol{\xi} \boldsymbol{M}_0 \boldsymbol{u}_{\varepsilon 1} - \lambda_2 \boldsymbol{\xi} \boldsymbol{M}_0 \boldsymbol{u}_{\varepsilon 2} - \sum_s \alpha_s \eta_s + \sum_{s,t} \delta_{st} \eta_s \eta_t + \sum_{s,t,u} \nu_{stu} \eta_s \eta_t \eta_u) \quad (g,\ l = 2,\ 3,\ 4,\ 6,\ 7,\ 8;\ r,\ s,\ t,\ u = 1,\ 2,\ \cdots,\ n) \tag{32}$$

where:

$$\begin{cases} \sum_s \alpha_s \eta_s = \boldsymbol{\xi} \boldsymbol{K}_{00} \boldsymbol{\eta} + \boldsymbol{\xi} \boldsymbol{\phi}^T \boldsymbol{M} \boldsymbol{u}_{\varepsilon 1} \boldsymbol{k}_{e1} \boldsymbol{\phi} \boldsymbol{\eta} + \boldsymbol{\xi} \boldsymbol{\phi}^T \boldsymbol{M} \boldsymbol{u}_{\varepsilon 2} \boldsymbol{k}_{\varepsilon 1} \boldsymbol{\phi} \boldsymbol{\eta} \\ \sum_{s,t} \delta_{st} \eta_s \eta_t = \sum_{n=1}^{8} \boldsymbol{\xi} \boldsymbol{\eta}^T \boldsymbol{G}_{0n} \boldsymbol{K}_{0n} \boldsymbol{\eta} + \frac{1}{2} \sum_{n=1}^{8} \boldsymbol{\xi} \boldsymbol{\eta}^T \boldsymbol{K}_{0n} \boldsymbol{\eta} \boldsymbol{G}_{0n} + \boldsymbol{\xi} \boldsymbol{\phi}^T \boldsymbol{M} \boldsymbol{u}_{\varepsilon 1} \boldsymbol{\phi}^T \boldsymbol{\eta}^T \boldsymbol{k}_{e2} \boldsymbol{\phi} \boldsymbol{\eta} + \boldsymbol{\xi} \boldsymbol{\phi}^T \boldsymbol{M} \boldsymbol{u}_{\varepsilon 2} \boldsymbol{\phi}^T \boldsymbol{\eta}^T \boldsymbol{k}_{\varepsilon 2} \boldsymbol{\phi} \boldsymbol{\eta} \\ \sum_{s,t,u} \nu_{stu} \eta_s \eta_t \eta_u = \frac{1}{2} \sum_g \sum_l \boldsymbol{\xi} \boldsymbol{\eta}^T \boldsymbol{G}_{0gl} \boldsymbol{\eta} \boldsymbol{K}_{0gl} \boldsymbol{\eta} + \frac{1}{2} \sum_g \sum_l \boldsymbol{\xi} \boldsymbol{G}_{0gl} \boldsymbol{\eta} \boldsymbol{\eta}^T \boldsymbol{K}_{0gl} \boldsymbol{\eta} \end{cases} \tag{33}$$

and α_s, δ_{st} and γ_{stu} are the coefficients of η_s, $\eta_s \eta_t$ and $\eta_s \eta_t \eta_u$ respectively.

The Multiple Scale perturbation Method (MSM) [10, 11] has been applied to the dynamic model nonlinear analysis. $n+1$ independent time scales are introduced as:

$$T_a = \varepsilon^a t, \quad (a = 0,\ 1,\ 2,\ \cdots,\ n). \tag{34}$$

The derivative about t can be transformed into the partial derivative expansions about T_a, namely:

$$\begin{cases} \frac{d}{dt} = D_0 + \varepsilon D_1 + \varepsilon^2 D_2 + \cdots \\ \frac{d^2}{dt^2} = D_0^2 + 2\varepsilon D_0 D_1 + \varepsilon^2 (D_1^2 + 2 D_0 D_2) + \cdots \end{cases} \tag{35}$$

where $D_r = \frac{\partial}{\partial T_r}$, $(r = 0,\ 1,\ 2,\ \cdots,\ n)$.

Substituting Eq. (35) into Eq. (32), and η_r can be expressed as $n+1$ function with the independent variable T_m and ε:

$$\eta_r = \eta_{r0}(T_0, T_1, \cdots, T_n) + \varepsilon \eta_{r1}(T_0, T_1, \cdots, T_n) + \varepsilon^2 \eta_{r2}(T_0, T_1, \cdots, T_n) + \cdots. \tag{36}$$

Taking approximate first-order solution of η_r, gained:

$$\eta_r = \eta_{r0}(T_0, T_1) + \varepsilon \eta_{r1}(T_0, T_1) \tag{37}$$

and:

$$\boldsymbol{\eta}_0 = \boldsymbol{\eta}_0(T_0, T_1) + \varepsilon \boldsymbol{\eta}_1(T_0, T_1). \tag{38}$$

Substituting Eq. (36) and (37) into Eq. (33), making the sum of coefficients of the same power of ε equal to zero, and:

$$D_0^2\eta_{r0}+\omega_r^2\eta_{r0}=P_{0r}+\sum_{f=1}^{8}\boldsymbol{F}_{0fr}, \tag{39}$$

$$\begin{aligned}D_0^2\eta_{r1}+\omega_r^2\eta_{r1}=&-2D_0D_1\eta_{r0}-2\zeta_r\omega_rD_0\eta_{r0}-\lambda_1\boldsymbol{\xi}\boldsymbol{M}_0\boldsymbol{u}_{\varepsilon 1}\\&-\lambda_2\boldsymbol{\xi}\boldsymbol{M}_0\boldsymbol{u}_{\varepsilon 2}-\sum_s\alpha_s\eta_{s0}+\sum_{s,t}\delta_{st}\eta_{s0}\eta_{t0}+\sum_{s,t,u}\nu_{stu}\eta_{s0}\eta_{t0}\eta_{u0}.\end{aligned} \tag{40}$$

Eq. (39) admits the solution:

$$\begin{aligned}\eta_{r0}=&A_r(T_1)\exp(i\omega_rT_0)+\sum_{k=1}^{m}[\Lambda_{1rk}\exp(ikv_1T_0)+\Lambda_{2rk}\exp(ikv_2T_0)\\&+\Lambda_{3rk}\exp(ikv_3T_0)+\Lambda_{4rk}\exp(ikv_4T_0)+\Lambda_{5rk}\exp(ikv_5T_0)\\&+\Lambda_{6rk}\exp(ikv_6T_0)+\Lambda_{7rk}\exp(ikv_7T_0)+\Lambda_{8rk}\exp(ikv_8T_0)]+cc\end{aligned} \tag{41}$$

where:

$$A_r=\frac{1}{2}a_r\exp(j\theta_r), \tag{42}$$

$$\Lambda_{prk}=\Gamma_{prk}\exp(i\tau_{pki}),\quad (p=1,\ 2,\ \cdots,\ 8). \tag{43}$$

and $\Gamma_{prk}=\dfrac{F_{0prk}}{2(\omega_r^2-k^2v_p^2)}$, a_r and θ_r can be resolved by the method of Newton-Raphson, ω_r is the *r*-order instantaneous natural frequency mean of the system.

Combination resonance analysis

The 2-DOF controllable close-chain linkage mechanism is a multi-frequency vibration system. Substituting Eq. (41) into Eq. (40), one can obtain that the combination resonance will take place in the system on the condition that $\omega_r\approx\left|\pm jv_p\pm kv_q\right|$ or $\omega_r\approx\left|\pm 2jv_p\pm kv_q\right|$. Here, the combination resonance properties of the system caused by the electromagnetic parameter excitations, which effected by the rotation frequencies of stator winding rotating magnetic field of servomotor and 3-phase AC motor, are analyzed when $2v_7+v_6\approx\omega_r$. Only the vibration eccentricity is considered in this paper, and the external force is ignored, namely $\boldsymbol{P}=\boldsymbol{0}$, the internal resonance is also ignored. The tuning parameter σ is introduced to make:

$$2v_7+v_6=\omega_r+\varepsilon\sigma,\quad \sigma=0(1). \tag{44}$$

Substituting Eqs. (41) and (44) into Eq. (40), and then the condition that the solution has no secular terms is:

$$-(2i\omega_rD_1A_r+2i\zeta_r\omega_r^2A_r)-\alpha_rA_r+3\nu_{rrr}\overline{A}_rA_rA_r+\sum_{s,t}\delta_{st}(\Lambda_{7s2}\Lambda_{6t1}+\Lambda_{7t2}\Lambda_{6s1})\exp(i\sigma T_1)$$

$$+\sum_{t,u}\nu_{rtu}(\sum_{k=1}^{m}\sum_{p=1}^{8}A_{\mathrm{r}}\Lambda_{ptk}\bar{\Lambda}_{puk}+\sum_{k=1}^{m}\sum_{p=1}^{8}A_{\mathrm{r}}\bar{\Lambda}_{ptk}\Lambda_{puk})+\sum_{s,u}\nu_{sru}(\sum_{k=1}^{m}\sum_{p=1}^{8}A_r\bar{\Lambda}_{psk}\Lambda_{puk}+\sum_{k=1}^{m}\sum_{p=1}^{8}A_r\Lambda_{psk}\bar{\Lambda}_{puk})$$
$$+\sum_{s,t}\nu_{str}(\sum_{k=1}^{m}\sum_{p=1}^{8}A_r\bar{\Lambda}_{psk}\Lambda_{ptk}+\sum_{k=1}^{m}\sum_{p=1}^{8}A_r\Lambda_{psk}\bar{\Lambda}_{ptk})+\sum_{t,u}\nu_{rtu}(\bar{A}_r\Lambda_{7t4}\Lambda_{6u2}+\bar{A}_r\Lambda_{7u4}\Lambda_{6t2})\exp(i2\sigma T_1)$$

$$+\sum_{s,u}\nu_{sru}(\bar{A}_r\Lambda_{7s4}\Lambda_{6u2}+\bar{A}_r\Lambda_{7u4}\Lambda_{6s2})\exp(i2\sigma T_1)+\sum_{s,t}\nu_{str}(\bar{A}_r\Lambda_{7s4}\Lambda_{6t2}+\bar{A}_r\Lambda_{7t4}\Lambda_{6s2})\exp(i2\sigma T_1)$$
$$+\sum_{s,t,u}\nu_{stu}(\Lambda_{7s1}\Lambda_{7t1}\Lambda_{6u1}+\Lambda_{7s1}\Lambda_{7u1}\Lambda_{6t1}+\Lambda_{7t1}\Lambda_{7u1}\Lambda_{6s1})\exp(i\sigma T_1)=0 \tag{45}$$

where α_r and ν_{stu} can be resolved from Eq. (32). Substituting Eqs. (42) and (43) into Eq. (45), we obtain:

$$-(i\omega_r\dot{a}_r-\omega_r a_r\dot{\theta}_r+i\zeta_r\omega_r^2 a_r)-\frac{1}{2}\alpha_r a_r+\frac{3}{8}\nu_{rrr}a_r^3$$
$$+\sum_{s,t}\delta_{st}[\Gamma_{7s2}\Gamma_{6t1}\exp i(\sigma T_1-\theta_r+\tau_{72s}+\tau_{61t})+\Gamma_{pt2}\Gamma_{qs1}\exp i(\sigma T_1-\theta_r+\tau_{61s}+\tau_{72t})]$$
$$+\sum_{s,t,u}\nu_{stu}[\Gamma_{7s1}\Gamma_{7t1}\Gamma_{6u1}\exp i(\sigma T_1-\theta_r+\tau_{71s}+\tau_{71t}+\tau_{61u})$$
$$+\Gamma_{7s1}\Gamma_{7u1}\Gamma_{6t1}\exp i(\sigma T_1-\theta_r+\tau_{71s}+\tau_{71u}+\tau_{61t})$$
$$+\Gamma_{7t1}\Gamma_{7u1}\Gamma_{6s1}\exp i(\sigma T_1-\theta_r+\tau_{71t}+\tau_{71u}+\tau_{61s})]$$
$$+\sum_{t,u}\nu_{rtu}[\sum_{k=1}^{m}\sum_{p=1}^{8}\frac{1}{2}a_r\Gamma_{ptk}\Gamma_{puk}\exp i(\tau_{pkt}-\tau_{pku})+\sum_{k=1}^{m}\sum_{p=1}^{8}\frac{1}{2}a_r\Gamma_{ptk}\Gamma_{puk}\exp i(-\tau_{pkt}+\tau_{pku})]$$
$$+\sum_{s,u}\nu_{sru}[\sum_{k=1}^{m}\sum_{p=1}^{8}\frac{1}{2}a_r\Gamma_{psk}\Gamma_{puk}\exp i(-\tau_{pks}+\tau_{pku})+\sum_{k=1}^{m}\sum_{p=1}^{8}\frac{1}{2}a_r\Gamma_{psk}\Gamma_{puk}\exp i(\tau_{pks}-\tau_{pku})]$$
$$+\sum_{s,t}\nu_{str}[\sum_{k=1}^{m}\sum_{p=1}^{8}\frac{1}{2}a_r\Gamma_{psk}\Gamma_{ptk}\exp i(-\tau_{pks}+\tau_{pkt})+\sum_{k=1}^{m}\sum_{p=1}^{8}\frac{1}{2}a_r\Lambda_{psk}\bar{\Lambda}_{ptk}\Gamma_{psk}\Gamma_{ptk}\exp i(\tau_{pks}-\tau_{pkt})]$$
$$+\sum_{t,u}\nu_{rtu}[\frac{1}{2}a_r\Gamma_{7t4}\Gamma_{6u2}\exp i(2\sigma T_1-2\theta_r+\tau_{74t}+\tau_{62u})+\frac{1}{2}a_r\Gamma_{7u4}\Gamma_{6t2}\exp i(2\sigma T_1-2\theta_r+\tau_{74u}+\tau_{62t})]$$
$$+\sum_{s,u}\nu_{sru}[\frac{1}{2}a_r\Gamma_{7s4}\Gamma_{6u2}\exp i(2\sigma T_1-2\theta_r+\tau_{74s}+\tau_{62u})+\frac{1}{2}a_r\Gamma_{7u4}\Gamma_{6s2}\exp i(2\sigma T_1-2\theta_r+\tau_{74u}+\tau_{62s})]$$
$$+\sum_{s,t}\nu_{str}[\frac{1}{2}a_r\Gamma_{7s4}\Gamma_{6t2}\exp i(2\sigma T_1-2\theta_r+\tau_{74s}+\tau_{62t})+\frac{1}{2}a_r\Gamma_{7t4}\Gamma_{6s2}\exp i(2\sigma T_1-2\theta_r+\tau_{74t}+\tau_{62s})]$$
$$=0. \tag{46}$$

Assuming:

$$\psi_r=3\sigma T_1-\theta_r. \tag{47}$$

Substituting Eq. (47) into Eq. (46), and separating the real part and the imaginary part:

$$-a_r\dot{\psi}_r=-a_r\sigma-\frac{1}{2\omega_r}\alpha_r a_r+\frac{3}{8\omega_r}\nu_{rrr}a_r^3+\frac{1}{\omega_r}\sum_{t,u}\sum_{k=1}^{m}\sum_{p=1}^{8}\nu_{rtu}a_r\Gamma_{ptk}\Gamma_{puk}\cos(\tau_{pkt}-\tau_{pku})$$

$$+\frac{1}{\omega_r}\sum_{s,t}\delta_{st}[\Gamma_{7s2}\Gamma_{6t1}\cos(\psi_r+\tau_{72s}+\tau_{61t})+\Gamma_{7t2}\Gamma_{6s1}\cos(\psi_r+\tau_{72t}+\tau_{61s})]$$

$$+\frac{1}{\omega_r}\sum_{s,t,u}\nu_{stu}[\Gamma_{7s1}\Gamma_{7t1}\Gamma_{6u1}\cos(\psi_r+\tau_{71s}+\tau_{71t}+\tau_{61u})$$

$$+\Gamma_{7s1}\Gamma_{7u1}\Gamma_{6t1}\cos(\psi_r+\tau_{71s}+\tau_{71u}+\tau_{61t})+\Gamma_{7t1}\Gamma_{7u1}\Gamma_{6s1}\cos(\psi_r+\tau_{71t}+\tau_{71u}+\tau_{61s})]$$

$$+\frac{1}{\omega_r}\sum_{s,u}\sum_{k=1}^{m}\sum_{p=1}^{8}\nu_{sru}a_r\Gamma_{psk}\Gamma_{puk}\cos(\tau_{pks}-\tau_{pku})+\frac{1}{\omega_r}\sum_{s,t}\sum_{k=1}^{m}\sum_{p=1}^{8}\nu_{str}a_r\Gamma_{psk}\Gamma_{ptk}\cos(\tau_{pks}-\tau_{pkt})$$

$$+\frac{1}{2\omega_r}\sum_{t,u}\nu_{rtu}[a_r\Gamma_{7t4}\Gamma_{6u2}\cos(2\psi_r+\tau_{74t}+\tau_{62u})+a_r\Gamma_{7u4}\Gamma_{6t2}\cos(2\psi_r+\tau_{74u}+\tau_{62t})]$$

$$+\frac{1}{2\omega_r}\sum_{s,u}\nu_{sru}[a_r\Gamma_{7s4}\Gamma_{6u2}\cos(2\psi_r+\tau_{74s}+\tau_{62u})+a_r\Gamma_{7u4}\Gamma_{6s2}\cos(2\psi_r+\tau_{74u}+\tau_{62s})]$$

$$+\frac{1}{2\omega_r}\sum_{s,t}\nu_{str}[a_r\Gamma_{7s4}\Gamma_{6t2}\cos(2\psi_r+\tau_{74s}+\tau_{62t})+a_r\Gamma_{7t4}\Gamma_{6s2}\cos(2\psi_r+\tau_{74t}+\tau_{62s})]. \quad (48)$$

$$\dot{a}_r=-\zeta_r\omega_r a_r+\frac{1}{\omega_r}\sum_{s,t}\delta_{st}[\Gamma_{7s2}\Gamma_{6t1}\sin(\psi_r+\tau_{72s}+\tau_{61t})+\Gamma_{7t2}\Gamma_{6s1}\sin(\psi_r+\tau_{72t}+\tau_{61s})]$$

$$+\frac{1}{\omega_r}\sum_{s,t,u}\nu_{stu}[\Gamma_{7s1}\Gamma_{7t1}\Gamma_{6u1}\sin(\psi_r+\tau_{71s}+\tau_{71t}+\tau_{61u})$$

$$+\Gamma_{7s1}\Gamma_{7u1}\Gamma_{6t1}\sin(\psi_r+\tau_{71s}+\tau_{71u}+\tau_{61t})$$

$$+\Gamma_{7t1}\Gamma_{7u1}\Gamma_{6s1}\sin(\psi_r+\tau_{71t}+\tau_{71u}+\tau_{61s})]$$

$$+\frac{1}{2\omega_r}\sum_{t,u}\nu_{rtu}[a_r\Gamma_{7t4}\Gamma_{6u2}\sin(2\psi_r+\tau_{74t}+\tau_{62u})+a_r\Gamma_{7u4}\Gamma_{6t2}\sin(2\psi_r+\tau_{74u}+\tau_{62t})]$$

$$+\frac{1}{2\omega_r}\sum_{s,u}\nu_{sru}[a_r\Gamma_{7s4}\Gamma_{6u2}\sin(2\psi_r+\tau_{74s}+\tau_{62u})+a_r\Gamma_{7u4}\Gamma_{6s2}\sin(2\psi_r+\tau_{74u}+\tau_{62s})]$$

$$+\frac{1}{2\omega_r}\sum_{s,t}\nu_{str}[a_r\Gamma_{7s4}\Gamma_{6t2}\sin(2\psi_r+\tau_{74s}+\tau_{62t})+a_r\Gamma_{7t4}\Gamma_{6s2}\sin(2\psi_r+\tau_{74t}+\tau_{62s})]. \quad (49)$$

Under the combination resonance mentioned above, the steady movement condition of system is:

$$\dot{a}_r=\dot{\psi}_r=0. \quad (50)$$

a_r and ψ_r can be resolved by the Newton-Raphson method. And substituting a_r and ψ_r into Eq. (41), the first order approximate steady solutions of combination resonance affected by electromagnetic parameter excitations when $2\nu_7+\nu_6\approx\omega_r$ can be obtained as follows:

$$\eta_{r0}=a_r\cos(\omega_r T_0-\psi_r)+\sum_{k=1}^{m}\sum_{p}F_{0prk}(\omega_r^2-k^2\nu_p^2)^{-1}\cos(\omega_r T_0+\tau_{pki})+O(\varepsilon). \quad (51)$$

Assuming that:

$$\left.\begin{aligned}a_r&=a_{r0}+\delta a_r\\ \psi_r&=\psi_{r0}+\delta\psi_r\end{aligned}\right\}. \quad (52)$$

Where a_{r0} and ψ_{r0} are the steady solutions with Eqs. (47), (48) and (49). Substituting Eq. (52) into Eqs. (47) and (48), and only reserving the linear terms of δa_r and $\delta\psi_r$, and the equation of variation around the singular point (a_{r0}, ψ_{r0}) can be obtained as:

$$\left.\begin{aligned}\frac{d(\delta a_r)}{dt} &= -\zeta_r\omega_r\delta a_r + [a_{r0}\sigma + \frac{1}{2\omega_r}\alpha_r a_{r0} - \frac{3}{8\omega_r}\nu_{rrr}a_{r0}^3 - b]\delta\psi_r \\ \frac{d(\delta\psi_r)}{dt} &= (\frac{3}{4\omega_r}\nu_{rrr}a_{r0} - \frac{1}{2\omega_r})\delta a_r - \zeta_r\omega_r\delta\psi_r\end{aligned}\right\}. \tag{53}$$

The coefficient matrix:

$$\begin{bmatrix} C_1 & C_2 \\ C_3 & C_4 \end{bmatrix} = \begin{bmatrix} -\zeta_r\omega_r & [a_{r0}\sigma + \frac{1}{2\omega_r}\alpha_r a_{r0} - \frac{3}{8\omega_r}\nu_{rrr}a_{r0}^3 - b] \\ \frac{3}{4\omega_r}\nu_{rrr}a_{r0} - \frac{1}{2\omega_r} & -\zeta_r\omega_r \end{bmatrix}. \tag{54}$$

The stability conditions are:

$$p \equiv -(C_1 + C_4) = 2\zeta_r\omega_r > 0 \tag{55}$$

and:

$$q \equiv (C_1C_4 - C_2C_3) = \zeta_r^2\omega_r^2 + (\frac{3}{4\omega_r}\nu_{rrr}a_{r0} - \frac{1}{2\omega_r})[a_{r0}\sigma + \frac{1}{2\omega_r}\alpha_r a_{r0} - \frac{3}{8\omega_r}\nu_{rrr}a_{r0}^3 - b] > 0 \tag{56}$$

where:

$$b = \frac{1}{\omega_r}\sum_{t,u}\sum_{k=1}^{m}\sum_{p=1}^{8}\nu_{rtu}a_{r0}\Gamma_{ptk}\Gamma_{puk}\cos(\tau_{pkt} - \tau_{pku})$$
$$-\frac{1}{\omega_r}\sum_{s,u}\sum_{k=1}^{m}\sum_{p=1}^{8}\nu_{sru}a_{r0}\Gamma_{psk}\Gamma_{puk}\cos(\tau_{pks} - \tau_{pku}) - \frac{1}{\omega_r}\sum_{s,t}\sum_{k=1}^{m}\sum_{p=1}^{8}\nu_{str}a_{r0}\Gamma_{psk}\Gamma_{ptk}\cos(\tau_{pks} - \tau_{pkt})$$

and σ can be solved from Eqs. (47), (48) and (49).

As shown in Eqs. (55) and (56), $p > 0$ always is to be sure as far as the positive damping system. Therefore, the stability of steady solution under the combination resonance caused by the two motors electromagnetic parameter excitations is related to the structural parameters, electromagnetic parameters of motor, damping ratio of system and phase angle of every excitation.

Experiment

Each link of the linkage mechanism is a homogeneous element. The width and thickness are 30 mm and 2 mm respectively. The lengths of each links are as follows: crank $L_1 = 200$ mm and $L_4 = 150$ mm, coupler $L_2 = L_3 = 400$ mm, and frame $L_5 = 400$ mm (Fig. 1). The material of link is aluminum: $\rho = 2700$ kg / m^3, $E = 70$ GPa. The lumped mass of the intersection

between the crank and the coupler is $m_{01} = 0.142$ kg. The lumped mass of the intersection between the two couplers is $m_{02} = 0.092$ kg. The controllable motor 1 is 90ZYT motor and motor 2 is YS8024 motor. The motors are custom-made by motor manufacturer. The parameters of motors are presented by the manufacturer. The experimental setup is provided in Fig. 4.

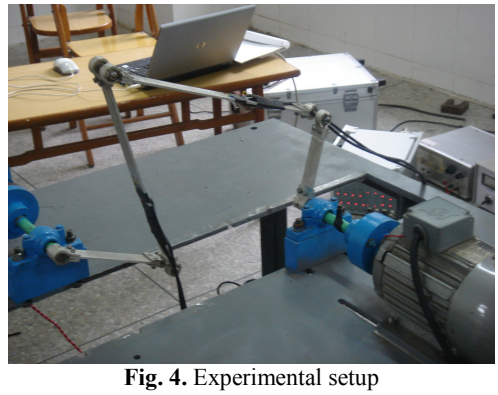

Fig. 4. Experimental setup

The parameters of the motors are as follows:

① The parameters of the control motor 1

The rated power of the 90ZYT motor $P_N = 0.75$ kW, the rated voltage $U_{kn} = 220$ V, the rated rotational speed of the motor is 1500 r / min, and the stall torque is 2.0 N·m. The static-geometric eccentricity of the motor $e_{01} = 0.75$ mm and the rotational eccentricity $\varepsilon_{01} = 0.5$ mm. The magnetic permeability coefficient of air $\mu_0 = 4\pi \times 10^{-7}$ H/m, the length of the even air-gap $\delta_0 = 0.25$ mm, and the saturation $k_\mu = 1.2$. The number of excitation windings of the motor $W = 924$ and the coefficient $K_w = 0.92$. The peak value of field current $I = 3.58$ A. The number of magnetic pole-pairs of the motor $p = 1$. $m_1 = 2$ and $m_2 = 2$ are the number of phases of the stator and rotor respectively. The reactance of field windings $x_m = 594.35$ Ω. The reduction value of resistance and equivalent self-induction reactance of rotor respectively are $r' = 27.24$ Ω and $x' = 0.0196$ Ω. The slide ratio $s_1 = 0.0713$. The control voltage $U_k = 26$ V. The mass of the rotor $m_0 = 2.2$ kg. The moment of inertia of the motor rotor $J_{01} = 0.018$ kg·m^2. The length of the motor shaft $l = 363$ mm ($l_1 = 130$ mm, $l_2 = 53$ mm, and $l_3 = 180$ mm), the effective length of the rotor $l_{01} = 140$ mm and the inner radius of the motor stator $R_{01} = 23$ mm.

② The parameters of the control motor 2

The rated power of the YS8024 motor $P_N = 0.75$ KW, the rated current $I_N = 3.48 / 2.01$ A, the rated voltage $U_{kn} = 220$ V, and the rated rotational speed $n_N = 1440$ r / min. The static-geometric eccentricity $e_{02} = 0.73$ mm and the rotational eccentricity $\varepsilon_{02} = 0.5$ mm. The magnetic permeability coefficient of air $\mu_0 = 4\pi \times 10^{-7}$ H/m, the length of the even air-gap $\delta_0 = 0.25$ mm, and the saturation $k_\mu = 1.2$. The number of excitation windings of the motor $W = 824$ and the coefficient $K_w = 1$. The peak value of field current $I = 3.58$ A. The number

of the magnetic pole-pair of compounded magnetic field $p=1$. $m_1=3$ and $m_2=0.5$ are the number of phases of the stator and rotor respectively. The slide ratio $s_2=0.15$. The mass of the motor rotor $m_0=2.93$ kg. The moment of inertia of the motor rotor $J_0=0.021\ \text{kg}\cdot\text{m}^2$. The length of the motor shaft $l=208$ mm ($l_1=100$ mm, $l_2=33$ mm, and $l_3=175$ mm), the effective length of the rotor $l_{02}=80$ mm and the inner radius of the motor stator $R_{02}=37.5$ mm.

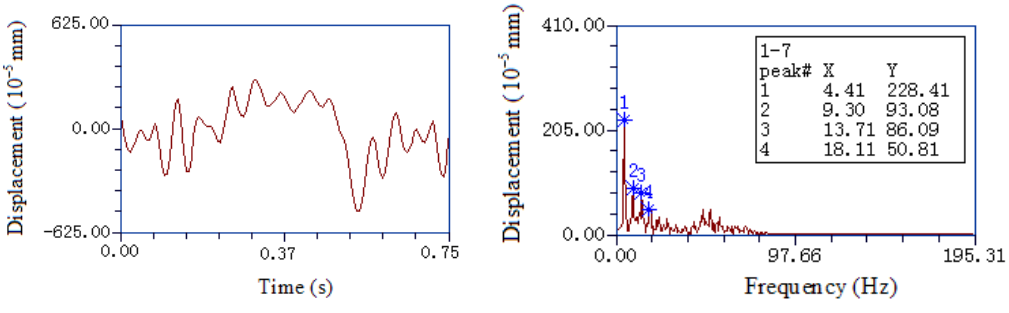

Fig. 5. Dynamic characteristics for the midpoint of link L_2

Given that the motor 1 nominal voltage is 26 V, nominal current is 0.05 A, rotational speed is 80 rpm, and the rotation frequency of stator winding rotating magnetic field is 1.3 Hz. The input voltage of motor 2 is 95 V, the rotational speed is 240 rpm, and the rotation frequency of stator winding rotating magnetic field is 4 Hz. The initial angles of the two cranks are 0° as shown in Fig. 1. The initial value of the vibration response is the one when the two cranks move to the initial position after the system come to stabilized state. Experimental time-domain and frequency-domain dynamic response characteristics of mid points of the links L_2 and L_3 in the direction perpendicular to the link axis are shown in Figs. 5-6. One may observe that there is a peak near the frequency $2v_6+v_7$. It was determined through analysis that the peak is mainly induced by the combination resonance caused by the two motors electromagnetic parameter excitations.

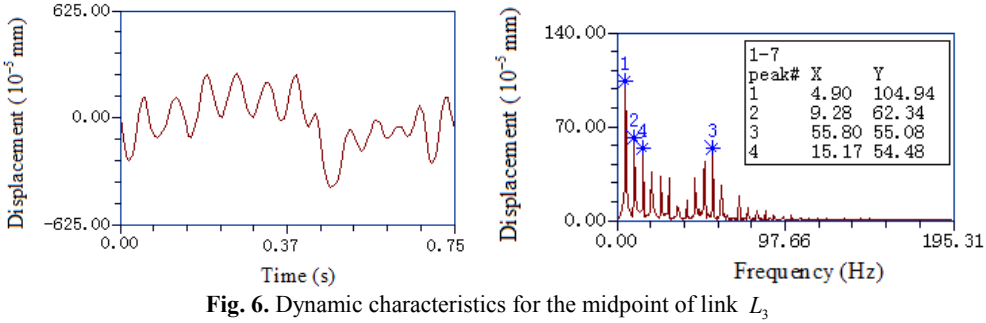

Fig. 6. Dynamic characteristics for the midpoint of link L_3

Conclusions

Nonlinear vibration of a controllable close-chain linkage mechanism was analyzed in this paper by considering the linkage mechanism and the controllable motors as an integrated system. Combination resonance properties of the close-chain linkage mechanism caused by

electromagnetic parameter excitations of the motors were analyzed by means of the multiple scales method. The study indicates that the combination resonance properties of the system are caused by the electromagnetic parameter excitations, which are influenced by the rotational frequencies of stator winding rotating magnetic field of the driving motors. It is demonstrated that not only the structural parameters, but also the electromagnetic parameters have significant effect on the combination resonance of the system. The work presented in this paper is beneficial to explaining some unexpected combination resonance phenomena occurring during high-speed operation of such multi-DOF controllable close-chain linkage mechanism.

Acknowledgements

These researches were supported by the National Natural Science Foundation of China (Grant No. 51265003), the Key Project of Chinese Ministry of Education (Grant No. 212133), the Guangxi Education Department Scientific Research Project (Grant No. 201203YB010) and the Guangxi Key Laboratory of Vehicle Parts Advanced Design and Manufacturing (Grant No. 2012KFMS07). We gratefully acknowledge the support agencies. Besides, we express our sincere thanks to the editors and the anonymous reviewers for their suggestions for the improvement of the paper.

Appendix

According to the finite element method, $W_1(x,t)$ and $V_1(x,t)$ can be expressed as:

$$\begin{cases} W_1(x,t)=\sum_i \chi_i(x)U_i(t), & i=1,2 \\ V_1(x,t)=\sum_i \chi_i(x)U_i(t), & i=3,4 \end{cases}$$

where $\chi_i(x)$ are the shape functions, and:

$$\chi_{1,2}(x)=\begin{cases} 1-10e_1^3+15e_1^4-6e_1^5, & x\le l_1 \\ 1-10e_2^3+15e_2^4-6e_2^5, & l_1<x\le l_1+l_2 \\ 0, & l_1+l_2<x\le l_1+l_2+l_3 \end{cases}$$

$$\chi_3(x)=\begin{cases} 0, & x\le l_1 \\ 1-e_2, & l_1<x\le l_1+l_2 \\ e_3, & l_1+l_2<x\le l_1+l_2+l_3 \end{cases}$$

$$\chi_4(x)=\begin{cases} 0, & x\le l_1 \\ 0, & l_1<x\le l_1+l_2 \\ 1-e_3, & l_1+l_2<x\le l_1+l_2+l_3 \end{cases}$$

where $e_1=\frac{x}{l_1}$, $e_2=\frac{l_1+l_2-x}{l_2}$, $e_3=\frac{l_1+l_2+l_3-x}{l_3}$, l_1, l_2 and l_3 are respectively the length between point 1 and point 2, point 2 and point 3, point 3 and point 4. $U_i(t)$ is the nodal displacement as shown in Fig. 2.

The mass matrix $\bar{\boldsymbol{M}}_1$ of the electromotor element is 4×4 matrix, and:

$$\begin{cases}(\bar{\boldsymbol{M}}_{\mathbf{1}})_{11}=\int_0^l m_1(x)\chi_1(x)\chi_1(x)dx\\(\bar{\boldsymbol{M}}_{\mathbf{1}})_{22}=\int_0^l m_1(x)\chi_2(x)\chi_2(x)dx\\(\bar{\boldsymbol{M}}_{\mathbf{1}})_{kp}=\int_0^l m_1(x)\chi_k(x)\chi_p(x)dx \qquad (k,\ p=3,\ 4)\end{cases}$$

where $m_1(x)$ is the mass distribution function of the servomotor shaft, including mass m_0 of the rotor. The other components of the mass matrix $\bar{\boldsymbol{M}}_{\mathbf{1}}$ are equal to zero.

The stiffness matrixes of the electromotor element are:

$$(\bar{\boldsymbol{K}}_{\mathbf{11}})_{11}=\int_0^l E_1I_1(x)[\frac{\partial^2\chi_1(x)}{\partial x^2}]^2dx,\ (\bar{\boldsymbol{K}}_{\mathbf{11}})_{12}=(\boldsymbol{K}_{\mathbf{11}})_{21}=\int_0^l E_1I_1(x)\frac{\partial\chi_1(x)}{\partial x}\frac{\partial\chi_2(x)}{\partial x}dx,$$

$$(\bar{\boldsymbol{K}}_{\mathbf{11}})_{22}=\int_0^l E_1I_1(x)[\frac{\partial^2\chi_2(x)}{\partial x^2}]^2dx,\ (\bar{\boldsymbol{K}}_{\mathbf{11}})_{kp}=\int_0^l G_1J_1(x)\frac{\partial\chi_k(x)}{\partial x}\cdot\frac{\partial\chi_p(x)}{\partial x}dx,\quad k,p=3,4,$$

$$\begin{aligned}(\bar{\boldsymbol{K}}_{\mathbf{12}})_{11}=&\frac{pR_{01}l_{01}\Lambda_{01}}{4\sigma_2^2}\int_0^{2\pi}\{(1+\cos 2\alpha)[F_{+s}\cos(\omega_{01}t-p\alpha)+F_{-s}\cos(\omega_{01}t+p\alpha)\\&+F_{+r}\cos(\omega_{01}t-p\alpha-\varphi_{10})+F_{-r}\cos(\omega_{01}t+p\alpha-\varphi_{20})]^2\}d\alpha,\end{aligned}$$

$$\begin{aligned}(\bar{\boldsymbol{K}}_{\mathbf{12}})_{12}=(\boldsymbol{K}_{\mathbf{12}})_{21}=&\frac{pR_{01}l_{01}\Lambda_{01}}{4\sigma_2^2}\int_0^{2\pi}\{(\sin 2\alpha)[F_{+s}\cos(\omega_{01}t-p\alpha)+F_{-s}\cos(\omega_{01}t+p\alpha)\\&+F_{+r}\cos(\omega_{01}t-p\alpha-\varphi_{10})+F_{-r}\cos(\omega_{01}t+p\alpha-\varphi_{20})]^2\}d\alpha,\end{aligned}$$

$$\begin{aligned}(\bar{\boldsymbol{K}}_{\mathbf{12}})_{22}=&\frac{pR_{01}l_{01}\Lambda_{01}}{4\sigma_2^2}\int_0^{2\pi}\{(1-\cos 2\alpha)[F_{+s}\cos(\omega_{01}t-p\alpha)+F_{-s}\cos(\omega_{01}t+p\alpha)\\&+F_{+r}\cos(\omega_{01}t-p\alpha-\varphi_{10})+F_{-r}\cos(\omega_{01}t+p\alpha-\varphi_{20})]^2\}d\alpha,\end{aligned}$$

$$(\bar{\boldsymbol{K}}_{\mathbf{12}})_{kp}=0,\qquad k,p=3,4,$$

$$\begin{aligned}&(\bar{\boldsymbol{K}}_{\mathbf{11}})_{13}=(\bar{\boldsymbol{K}}_{\mathbf{11}})_{14}=(\bar{\boldsymbol{K}}_{\mathbf{11}})_{23}=(\bar{\boldsymbol{K}}_{\mathbf{11}})_{24}=(\bar{\boldsymbol{K}}_{\mathbf{11}})_{31}=(\bar{\boldsymbol{K}}_{\mathbf{11}})_{32}=(\bar{\boldsymbol{K}}_{\mathbf{11}})_{41}=(\bar{\boldsymbol{K}}_{\mathbf{11}})_{42}\\&=(\bar{\boldsymbol{K}}_{\mathbf{12}})_{13}=(\bar{\boldsymbol{K}}_{\mathbf{12}})_{14}=(\bar{\boldsymbol{K}}_{\mathbf{12}})_{23}=(\bar{\boldsymbol{K}}_{\mathbf{12}})_{24}=(\bar{\boldsymbol{K}}_{\mathbf{12}})_{31}=(\bar{\boldsymbol{K}}_{\mathbf{12}})_{32}=(\bar{\boldsymbol{K}}_{\mathbf{12}})_{41}=(\bar{\boldsymbol{K}}_{\mathbf{12}})_{42}=0,\end{aligned}$$

$$\begin{aligned}(\bar{\boldsymbol{k}}_{01})_1=&\frac{pR_{01}l_{01}\Lambda_{01}}{2\sigma}\int_0^{2\pi}\{(\cos\alpha)[F_{+s}\cos(\omega_{01}t-p\alpha)+F_{-s}\cos(\omega_{01}t+p\alpha)\\&+F_{+r}\cos(\omega_{01}t-p\alpha-\varphi_{10})+F_{-r}\cos(\omega_{01}t+p\alpha-\varphi_{20})]^2\}d\alpha,\end{aligned}$$

$$\begin{aligned}(\bar{\boldsymbol{k}}_{01})_2=&\frac{pR_{01}l_{01}\Lambda_{01}}{2\sigma}\int_0^{2\pi}\{(\sin\alpha)[F_{+s}\cos(\omega_{01}t-p\alpha)+F_{-s}\cos(\omega_{01}t+p\alpha)\\&+F_{+r}\cos(\omega_{01}t-p\alpha-\varphi_{10})+F_{-r}\cos(\omega_{01}t+p\alpha-\varphi_{20})]^2\}d\alpha,\end{aligned}$$

$$(\bar{\boldsymbol{k}}_{01})_3=(\bar{\boldsymbol{k}}_{01})_4=0,$$

where E_1 is the modulus of elasticity of the servormotor shaft materials, $I_1(x)$ is the moment of inertia distribution function, G_1 is shear modulus of the servormotor shaft materials, $J_1(x)$ is the polar moment of inertia distribution function of the servormotor shaft.

Similarly, for the 3-phase AC motor element, the mass matrix $\bar{\boldsymbol{M}}_{\mathbf{2}}$ is 4×4 matrix, and:

$$\begin{cases}(\bar{\boldsymbol{M}}_{\mathbf{2}})_{11}=\int_0^{l'} m_2(x)\chi_1(x)\chi_1(x)dx\\(\bar{\boldsymbol{M}}_{\mathbf{2}})_{22}=\int_0^{l'} m_2(x)\chi_2(x)\chi_2(x)dx\\(\bar{\boldsymbol{M}}_{\mathbf{2}})_{kp}=\int_0^{l'} m_2(x)\chi_k(x)\chi_p(x)dx \quad k,p=3,4\end{cases}$$

The stiffness matrixes are:

$$\begin{cases}(\bar{\boldsymbol{K}}_{\boldsymbol{21}})_{11}=\int_0^{l'}E_2I_2(x)[\dfrac{\partial^2\chi_1(x)}{\partial x^2}]^2dx\\(\bar{\boldsymbol{K}}_{\boldsymbol{21}})_{22}=\int_0^{l'}E_2I_2(x)[\dfrac{\partial^2\chi_2(x)}{\partial x^2}]^2dx\\(\bar{\boldsymbol{K}}_{\boldsymbol{21}})_{kp}=\int_0^{l'}G_2J_2(x)\dfrac{\partial\chi_k(x)}{\partial x}\cdot\dfrac{\partial\chi_p(x)}{\partial x}dx\quad k,p=3,4\\(\bar{\boldsymbol{K}}_{\boldsymbol{21}})_{12}=(\bar{\boldsymbol{K}}_{\boldsymbol{21}})_{13}=(\bar{\boldsymbol{K}}_{\boldsymbol{21}})_{14}=(\bar{\boldsymbol{K}}_{\boldsymbol{21}})_{21}=(\bar{\boldsymbol{K}}_{\boldsymbol{21}})_{23}=(\bar{\boldsymbol{K}}_{\boldsymbol{21}})_{24}=(\bar{\boldsymbol{K}}_{\boldsymbol{21}})_{31}=(\bar{\boldsymbol{K}}_{\boldsymbol{21}})_{32}\\\quad=(\bar{\boldsymbol{K}}_{\boldsymbol{21}})_{41}=(\bar{\boldsymbol{K}}_{\boldsymbol{21}})_{42}=0\end{cases}$$

$$\begin{cases}(\bar{\boldsymbol{K}}_{\boldsymbol{22}})_{11}=-2h_1-h_2\cos(2\omega_{02}t)-h_3\sin(2\omega_{02}t)\\(\bar{\boldsymbol{K}}_{\boldsymbol{22}})_{12}=(\boldsymbol{K}_{\boldsymbol{22}})_{21}=-h_2\sin(2\omega_{02}t)+h_3\cos 2(\omega_{02}t)\\(\bar{\boldsymbol{K}}_{\boldsymbol{22}})_{22}=-2h_1+h_2\cos(2\omega_{02}t)+h_3\sin(2\omega_{02}t)\\(\bar{\boldsymbol{K}}_{\boldsymbol{22}})_{13}=(\bar{\boldsymbol{K}}_{\boldsymbol{22}})_{14}=(\bar{\boldsymbol{K}}_{\boldsymbol{22}})_{23}=(\bar{\boldsymbol{K}}_{\boldsymbol{22}})_{24}=(\bar{\boldsymbol{K}}_{\boldsymbol{22}})_{31}=(\bar{\boldsymbol{K}}_{\boldsymbol{22}})_{32}=(\bar{\boldsymbol{K}}_{\boldsymbol{22}})_{33}\\\quad=(\bar{\boldsymbol{K}}_{\boldsymbol{22}})_{34}=(\bar{\boldsymbol{K}}_{\boldsymbol{22}})_{41}=(\bar{\boldsymbol{K}}_{\boldsymbol{22}})_{42}=(\bar{\boldsymbol{K}}_{\boldsymbol{22}})_{43}=(\bar{\boldsymbol{K}}_{\boldsymbol{22}})_{44}=0\end{cases}$$

$$(\bar{\boldsymbol{k}}_{02})_1=\frac{R_{02}L_{02}\Lambda_{02}}{2}\int_0^{2\pi}\{(\cos\alpha)[F_{1m}\cos(\omega_{02}t-\alpha)+F_{2m}\cos(\beta_4+s_2\omega_{02}t-\alpha-\varphi)]^2\}d\alpha\ ,$$

$$(\bar{\boldsymbol{k}}_{02})_2=\frac{R_{02}L_{02}\Lambda_{02}}{2}\int_0^{2\pi}\{(\sin\alpha)[F_{1m}\cos(\omega_{02}t-\alpha)+F_{2m}\cos(\beta_4+s_2\omega_{02}t-\alpha-\varphi)]^2\}d\alpha\ ,$$

$$(\bar{\boldsymbol{k}}_{02})_3=(\bar{\boldsymbol{k}}_{02})_4=0\ ,$$

where:

$$\begin{cases}h_1=\dfrac{\pi R_{02}L_{02}\Lambda_{02}}{4\sigma_2^2}[{F_{1m}}^2+{F_{2m}}^2+2F_{1m}F_{2m}\cos\varphi]\\h_2=\dfrac{\pi R_{02}L_{02}\Lambda_{02}}{4\sigma_2^2}[{F_{1m}}^2+{F_{2m}}^2\cos(2\varphi)+2F_{1m}F_{2m}\cos\varphi]\\h_3=\dfrac{\pi R_{02}L_{02}\Lambda_{02}}{4\sigma_2^2}[{F_{2m}}^2\sin(2\varphi)+2F_{1m}F_{2m}\sin\varphi]\end{cases}$$

and E_2 is the modulus of elasticity of the 3-phase AC motor shaft materials, $I_2(x)$ is the moment of inertia distribution function of the 3-phase AC motor, G_2 is the shear modulus of the material of the 3-phase AC motor shaft, $J_2(x)$ is the polar moment of inertia distribution function of the 3-phase AC motor, ω_{02} is the synchronous speed of the 3-phase AC motor.

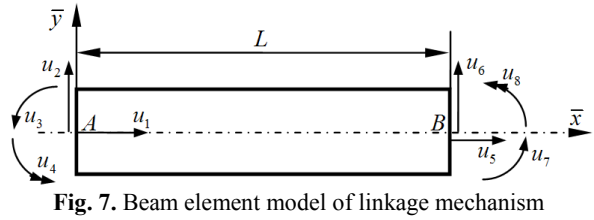

Fig. 7. Beam element model of linkage mechanism

In general, the links of the 2-DOF controllable linkage mechanism are slim bars, so they adapt to be simulated using beam element as shown in Fig. 7. In dynamic analysis of the beam element, the coupling terms of the elastic motion and the rigid body motion in the Coriolis acceleration and transport acceleration are neglected in studying the absolute acceleration of any point in the beam element. In calculation of strain energy, the shearing deformation energy and yield deformation energy are also omitted. The material of the link is adopted as metal. According to the finite element method, the longitudinal displacement $V_3(\bar{x},t)$ and the transversal displacement $W_3(\bar{x},t)$ of any point in the beam element can be expressed as:

$$\begin{cases} V_3(\bar{x},t) = \sum_i \gamma_i(\bar{x}) u_i(t) & (i = 1,5) \\ W_3(\bar{x},t) = \sum_i \gamma_i(\bar{x}) u_i(t) & (i = 2,3,4,6,7,8) \end{cases}$$

where $\bar{x}$ is the coordinate of beam element in local coordinate system, and the shape functions are as follows:

$\gamma_1(\bar{x}) = 1 - e$,

$\gamma_2(\bar{x}) = 1 - 10e^3 + 15e^4 - 6e^5$,

$\gamma_3(\bar{x}) = L \times (e - 6e^3 + 8e^4 - 3e^5)$,

$\gamma_4(\bar{x}) = L^2 \times (e^2 - 3e^3 + 3e^4 - 5e^5)/2$,

$\gamma_5(\bar{x}) = e$,

$\gamma_6(\bar{x}) = 10e^3 - 15e^4 + 6e^5$,

$\gamma_7(\bar{x}) = L \times (-4e^3 + 7e^4 - 3e^5)$,

$\gamma_8(\bar{x}) = L^2 \times (e^3 - 2e^4 + e^5)/2$,

where $e = \dfrac{\bar{x}}{L}$, L is the length of the beam element.

The mass matrix and stiffness matrix of the beam element are as follows:

$$\begin{cases} (\bar{\boldsymbol{M}}_3)_{ij} = \rho A(\bar{x}) \int_0^L \gamma_i(\bar{x}) \gamma_j(\bar{x}) d\bar{x} + \rho I \int_0^L \gamma_i'(\bar{x}) \gamma_j'(\bar{x}) d\bar{x}, & (i,j = 2,3,4,6,7,8) \\ (\bar{\boldsymbol{M}}_3)_{ij} = \rho A(\bar{x}) \int_0^L \gamma_i(\bar{x}) \gamma_j(\bar{x}) d\bar{x}, & (i,j = 1,5) \end{cases}$$

$$\begin{cases} (\bar{\boldsymbol{K}}_3)_{ij} = EJ(\bar{x}) \int_0^L \gamma_i''(\bar{x}) \gamma_j''(\bar{x}) d\bar{x}, & (i,j = 2,3,4,6,7,8) \\ (\bar{\boldsymbol{K}}_3)_{kp} = EA(\bar{x}) \int_0^L \gamma_k'(\bar{x}) \gamma_p'(\bar{x}) d\bar{x}, & (k,p = 1,5) \end{cases}$$

where I is the moment of inertia of cross-section.

The positive-sequence and negative-sequence components of the magnetomotive amplitude of stator and rotor of the servomotor (motor 1) respectively are:

$$\begin{cases} F_{+s} = \dfrac{1}{2}(1 + a_e) F_m \\ F_{-s} = \dfrac{1}{2}(1 - a_e) F_m \end{cases}$$

$$\begin{cases} F_{+r} = \dfrac{1}{2}\dfrac{m_2}{m_1}\dfrac{x_m}{\sqrt{(r'/s)^2 + (x')^2}}(1+a_e)F_m \\ F_{-r} = \dfrac{1}{2}\dfrac{m_2}{m_1}\dfrac{x_m}{\sqrt{[r'/(2-s)]^2 + (x')^2}}(1-a_e)F_m \end{cases}$$

where $F_m = 0.9\dfrac{WK_w}{p}I$, W is the number of turns of field winding, K_w is the coefficient of field winding, p is the number of pole-pairs, I is the peak value of field current. $a_e = \dfrac{U_k}{U_{kn}}$ is the effective signal coefficient, U_{kn} is the rated voltage and U_k is the actual control voltage. m_1 and m_2 are the number of phases of the stator and rotor respectively, x_m is the reactance of field windings, r' and x' are respectively the reduction value of resistance and equivalent self-induction reactance of rotor windings, the slip ratio s is the difference between the rotor speed and forward revolving field. $2-s$ is the slip ratio between the rotor speed and backward revolving field.

References

[1] **Ouyang P. R., Li Q., Zhang W. J.** Design, modeling and control of a hybrid machine system. Mechatronics, Vol. 14, Issue 4, 2004, p. 1197-1217.

[2] **Yao W., Cannella F., Dai J. S.** Automatic folding of cartons using a reconfigurable robotic system. Robotics and Computer-Integrated Manufacturing, Issue 27, 2011, p. 604-613.

[3] **Liou F. W., Arthur G. Erdman, Lin C. S.** Dynamic analysis of a motor-gear-mechanism system. Mechanism and Machine Theory, Vol. 26, Issue 3, 1991, p. 239-252.

[4] **Smaili A., Kopparapu M., Sannah M.** Elastodynamic response of a d. c. motor driven flexible mechanism system with compliant drive train components during start-up. Mechanism and Machine Theory, Vol. 31, Issue 5, 1996, p. 659-672.

[5] **Liu J., Zhang C.** Dynamic analysis of a motor-elastic linkage system. Journal of Tianjin University, Vol. 32, Issue 3, 1999, p. 265-269.

[6] **Li Z., Cai G., Huang Q., Liu S.** Analysis of nonlinear vibration of a motor–linkage mechanism system with composite links. Journal of Sound and Vibration, Issue 311, 2008, p. 924-940.

[7] **Wang R., Cai G., Zhou X.** An evolutionary analytic method of multi-DOF nonlinear coupling dynamic model for controllable close-chain linkage mechanism system. Mathematical Problems in Engineering, 2011, p. 1-17, DOI: 10.1155/2011/254547.

[8] **Wang R., Cai G., Lu H.** Electromechanical coupling equation and responses of the 2-DOF controllable linkage mechanism system. Journal of Mechanical Strength, Vol. 29, Issue 3, 2007, p. 356-364.

[9] **Qiu J.** Electromechanical Analysis Dynamics. Science Press, Beijing, 1997.

[10] **Nayfeh A. H., D. Mook T.** Nonlinear Oscillations. Wiley, New York, 1979.

[11] **Luongo A., Zulli D., Piccardo G.** Analytical and numerical approaches to nonlinear galloping of internally resonant suspended cables. Journal of Sound and Vibration, Issue 315, 2008, p. 375-393.